RAPID ISOLATION OF TARGET BACTERIA

FROM COMPLEX MATRICES

A Thesis

presented to

the Faculty of the Graduate School

at the University of Missouri

In Partial Fulfillment

of the Requirements for the Degree

Master of Science

---

by

JINWANG TAN

Dr. Shramik Sengupta, Thesis Supervisor

JULY 2010

The undersigned, appointed by the dean of the Graduate School, have examined the thesis entitled

RAPID ISOLATION OF TARGET BACTERIA

FROM COMPLEX MATRICES

presented by Jinwang Tan,

a candidate for the degree of Master of Science,

and hereby certify that, in their opinion, it is worthy of acceptance.

Shramik Sengupta, PhD, Biological Engineering

Luis Polo-Prada, PhD, Medical Pharmacology and Physiology

Liqun (Andrew) Gu, PhD, Biological Engineering

ACKNOWLEDGEMENTS

At first, I would like to give my special thanks to my supervisor, Dr. Shramik Sengupta, for his nice and helpful support in my two years study.

I also thank my lab group for supporting me on this project. Ms. Sachidevi Puttaswamy, Ms. Neha Gujarati, Ms. Shreya Ghoshdastidar, and Mr. Byungdoo Lee.

I am grateful to my committee members: Dr. Shramik Sengupta, Dr. Liqun Gu, Dr. Luis Polo-Prada. They gave me suggestions and advised me in my research.

Finally, I owe a special note of thanks to my father, Shilian Tan, mother, Youping Zhang for their support.

TABLE OF CONTENTS

LIST OF FIGURES

LIST OF TABLES

Table Page

RAPID ISOLATION OF TARGET BACTERIA

FROM COMPLEX MATRICES

Jinwang Tan

Dr. Shramik Sengupta, Thesis Supervisor

ABSTRACT

The long term goal of the research effort in our group was to develop a new rapid diagnostic process for sepsis. The specific project described in this work aims to obtain these “pure” isolates of the infectious bacteria within a total time of less than 1.5 hours. The proposed isolation process consists of 2 steps: (a) a novel kinetically limited density differential centrifugation step that serves as a “coarse” method, and (b): a dielectrophoresis (DEP) based sorting technique that serves as a “polishing” step.

Kinetically Limited Density Differential Centrifugation enables us to convert a mixture in which the bacteria are an extremely small fraction of the particles to a suspension where bacteria constitute the majority of the particles. It is expected that the sample yielded by this separation technique can be “polished” using flow through dielectrophoresis (DEP). We also measured the DEP properties of target bacteria and RBC to determine the experiment condition for further purification. Besides that, we designed and fabricated the MEMS device for Flow-Through Dielectrophoresis (DEP) to obtain pure isolates of bacteria.

CHAPTER 1

INTRODUCTION

1.1. Specific aims

The long term goal of the research effort in our group was to develop a new diagnostic process that will aid in the management of sepsis by (a) detecting viable bacteria in blood samples (if present) within 2-12 hours with a sensitivity and specificity of >98% (b) isolating and identifying these bacteria within an additional 2 hours with an accuracy of > 95%, and (c) establishing their antibiotic susceptibility profiles within 6 hours. Using current technology, it takes 1-5 days to detect the presence of viable bacteria in blood, approximately 1 day to identify the bacteria, and an additional 2-5 days to obtain the antibiotic susceptibility profile.

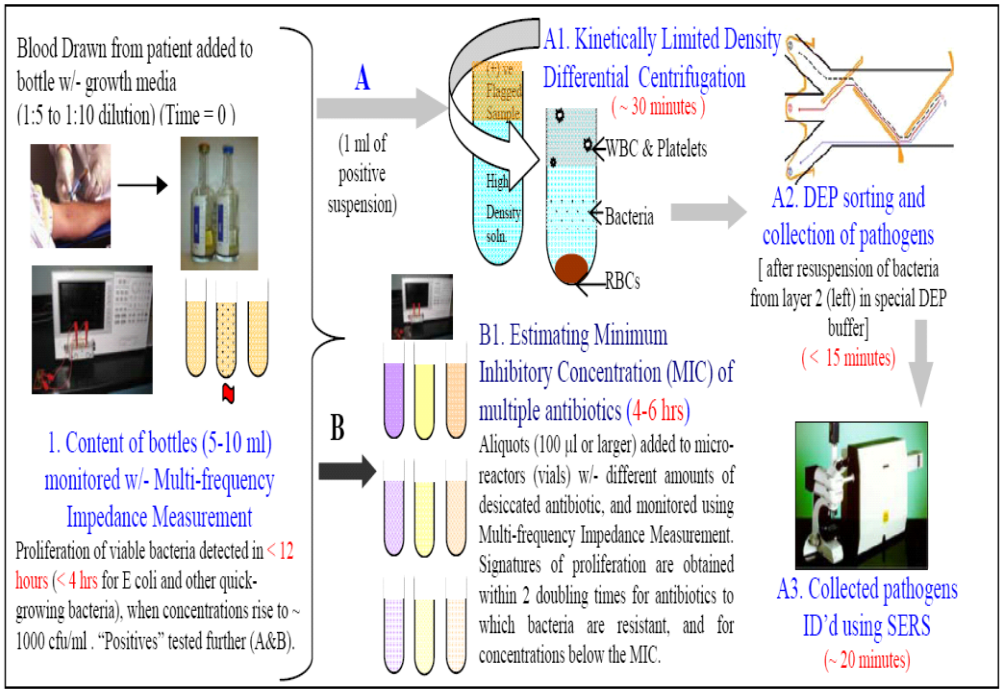

Figure 1.1 Outline of proposed diagnostic process

In this specific project, we attempted to realize the steps A1 and A2 of the figure above. These steps enabled us to obtain "pure" isolates of the infectious bacteria within a total time of less than 1.5 hours. Once "pure" isolates were obtained, the identity of the bacteria can then be obtained using Surface Enhanced Raman Spectroscopy (SERS) in less than 20 minutes. The proposed isolation process consists of 2 steps: (a) a novel Kinetically Limited Density Differential Centrifugation step that serves as a "coarse" method, and (b): a dielectrophoresis (DEP) based sorting technique that serves as a "polishing" step.

The proposed specific aims are:

1. To use Kinetically Limited Density Deference Centrifugation to isolate bacteria from (a) positive blood culture samples; (b) from whole blood. For current blood culture systems, at the time the culture turns "positive", there are about $10^6 – 10^7$ bacteria present in the growth suspension. The growth suspension consists of blood diluted in a 1:5 to 1:10 ratio into a microbiological growth medium containing proteins, salts, sugars etc. (Blood itself is a complex matrix consisting of ~10^9 red blood cells (RBC), ~10^7 white blood cells (WBC), ~10^8 platelets and plasma). Using the more advanced method being developed in our group, the samples can be flagged positive as soon as the bacteria concentration has risen to ~ 1000 CFU/ml. We will thus examine the feasibility of our system to obtain a relatively pure sample of bacteria from samples where the bacteria concentration lies within these two limits

2. Measure the DEP properties of target bacteria and RBC to determine the experiment condition for further purification.

3. Design and fabricate the MEMS device for Flow Through Dielectrophoresis (DEP) to obtain pure isolates of bacteria.

1.2. Background and significance

1.2.1. Epidemiology of sepsis

Sepsis is a disease which is an inflammatory response to microbes in blood, lungs, or other tissues that are sterile under normal circumstances. Sepsis can originate anywhere bacteria enters the human body, but since almost all tissues are washed by blood, this usually also leads to blood infection (septicemia). During infection, bacteria can produce and release complex molecules, which can provoke a dramatic response by the immune system. It can lead to septic shock, multiple organ dysfunction syndrome and death. Most of the sepsis cases are caused by *E coli*, *P. aeruginosa, Klebsiella* etc. It has been estimated (Angus and others 2001) that each year in the US, over 751,000 cases of severe sepsis occurs, out of which 383,000 (51.1%) require intensive care, and 215,000 (28.6%) are fatal. Other estimates (Wenzel and Edmond 2001) are lower (about 105,000 deaths each year). To put the numbers in perspective: even assuming that the lower estimate is correct, about 3 times as many people die from sepsis than from breast cancer.

Current technologies to detect such few bacteria in blood generally take 2 to 5 days to get the results. Unfortunately, patients who suffer sepsis may turn to organ dysfunction and low blood pressure during that time. In the past 3 decades, the ~30% mortality rate of sepsis has remained essentially unchanged. Numerous studies (Doern and others

1994; Kang and others 2003) have pointed out that the quicker one can detect the presence of bacteria in the blood, and identify the best antibiotic to be used, with the more successful one being able to reduce mortality.

1.2.2. Current clinical diagnostic protocol and technology

When a patient exhibits symptoms suggesting sepsis, clinicians call for a blood culture to check the presence of pathogens in the patient's blood. Blood is drawn from the patient, inoculated into a bottle containing growth medium, and the suspension (blood + growth medium) is incubated. Automated Blood Culture Systems (such as the BACTEC™, BacT/Alert™ and Vitek™) are used to monitor the bottle round-the-clock. These systems look for changes to the composition of the suspension (O_2 / CO_2 levels, pH etc.) brought about by bacterial metabolism.

If changes are detected, the bottle in question is flagged as positive. For many of the commonly occurring bacteria such as *E coli, Pseudomonos, Group B Streptococci*, etc., it usually takes 12-24 hours for bottles to turn positive. If the initial load of bacteria in the blood drawn is low (< 10 CFU/ml), it may take longer (even up to 72 hours). Though the practice is to keep the culture running for 120 hours (5 days) before deeming it to be negative, if the culture remains negative after 72 hours (3 days), it is unlikely to turn positive over the next couple of days.

If a positive result is obtained from the blood culture, the clinician typically orders the administration of broad-spectrum antibiotics. Once information on the identity of the infectious agent (bacteria) is available, more effective antibiotics can be administered. Currently, semi automated Microbial Identification Systems (MIS) exist (such as the Biolog^{TM}) that can run a large number of reactions in micro-titer wells, and depending on the levels of growth observed in each of them, predict the identity of the infective bacteria (based on information stored in its database). Typically, these systems require that the bacteria isolated from the blood culture to be grown on their specially designed nutrient agar for 18-24 hours, isolated from colonies suspended at particular densities in specially formulated buffers, and then loaded into their titer wells (where they are incubated for 4 -24 hours). Thus, an additional 1-2 days typically elapse before the clinician can get information regarding the identity of the bacteria.

1.2.3. Other technologies in development for detecting and identifying

There are a number of other efforts to develop improved culture-based technologies. Most of these technologies aim to develop more sensitive O_2, CO_2, pH or thermal sensors (Sengupta and others 2009). However, as we explain later (in Section 2.1.1), the long Times to Positivity (TTPs) that are observed for the BACTEC^{TM}, BacT/Alert^{TM} etc when initial bacterial loads are low, arise from fundamental limitations in the bacterial

metabolism rate. Yang and co-workers (Yang and others 2005) have tried to cut down TTPs by pre-concentrating the bacteria using dielectrophoresis (DEP) prior to culture. But because their method requires the suspension handled to pass through micro-channels only 10 micron deep, and the electric field needed for corralling the bacteria selectively from other particles is partially disrupted if there are too many other particles present, their method is applicable only to suspensions with “low” volume fractions of dispersed solids (largely clear suspensions such as water, growth media, or apple juice). In addition, there are other drawbacks, including potential inactivation of bacteria in high strength electric fields and less than stellar capture efficiencies that may lead to false negatives.

Over the last decade, considerable effort has been directed towards developing DNA based, and other molecular, non-culture based methods for the diagnosis of Sepsis. These were recently reviewed by Mancini. (Mancini and others 2010) As reported, Polymerase Chain Reaction (PCR) based methods (including Real Time PCR) suffer from four major drawbacks: (a) human DNA / RNA, which is present at much higher levels relative to bacterial DNA in blood samples, interferes with the extraction and amplification of the latter. Thus, the number of bacteria (amount of bacterial DNA) that needs to be present for these techniques to be able to detect them (the detection limit) is fairly high ($> 10^4$ CFU/ml); (b) presence of PCR inhibitors in the blood sample, leading to false negatives; (c) presence of contaminant bacterial DNA in reagents used, leading

to false positives (sterilization of reagents kills any bacteria present, but does not always eliminate DNA present); and (d) the risk of carryover contamination among samples in the same extraction round.

A significant amount of research has been devoted to overcoming these obstacles, with varying degrees of success. The use of ultra-pure chemicals and high-quality packaging in single-use doses can limit the extent of contamination of chemicals by bacterial DNA. Also, proteinases included among the reagents can degrade some of the PCR inhibitors present, and the use of automated systems with single use conduits and reactors can reduce carryover contamination to an extent. Finally, the amount of human DNA can be reduced prior to analysis either by selective digestion by enzymes, or by physical methods like affinity chromatography. Using combinations of the above, it is now quite readily feasible to use RT-PCR to identify bacteria in blood culture bottles that have been flagged positive. (Typically, by the time the culture bottles have been flagged positive, the concentration of bacteria there has risen to > 10^6 CFU/ml.) There are in fact, a number of technologies already on the market that do so – such as the PNA-FSH (AdvanDX, Woburn, MA), Hyplex BloodScreen (BAG, Germany), “Prove it Sepsis” (Mobidiag, Finland) etc, and their turnaround time is approximately 3 hours. There has also been some success in trying to detect the bacteria directly from blood, with three technologies having recently obtained licenses in Europe. The first, called Septi-Test (Molzym, Bremen, Germany) is a broad-range PCR-based assay targeting the 16S rRNA

genes of bacteria. It has a few major drawbacks: a detection limit of 20-40 CFU/ml (in many cases, the bacterial load in the blood may be as low as ~ 1 CFU/ml), a relatively long turn-around time of 8-12 hours (that is not that much faster than culture), and being prone to provide large number of false positives due to the influence of contaminating DNA. The second, called Vyoo (SIRS-Lab, Jena, Germany) is a multiplex PCR-based assay addressing approximately 35 bacterial species, and certain genes that confer antibiotic resistance such as *mecA, vanA, vanB* and *vanC*. Like the Septi-test, however, it is also reportedly prone to giving false positives due to contamination, but has a lower detection limit (3-10 CFU/ml as claimed by the company), and a shorter turnaround time (~8 hours). The most promising system of this type is the Septi-Fast system from Roche Diagnostics, which claims to offer results as quickly as 6 hours (but may take longer, depending on the sample). By using a disposable cassette with integrated reagent reservoirs, mechanisms for dispensing reagents and performing RT-PCR, it greatly reduces the false positives that plague the other two. Its major drawback is that it is able to detect just 25 common pathogens, and the detection limit varies from 3 - 30 CFU/ml, depending on the pathogen (that may, in many cases, be insufficient to detect pathogens). Also, the special manufacturing processes and the high purity of chemicals used in an attempt to eliminate stray bacterial DNA makes it a very costly test to perform (~ $215 - 290 per test, compared to ~ $20 per test for automated blood cultures using the BACTEC or BacT/Alert).

Besides the high detection limits (that result in false negatives), contamination issues (that result in false positives) and high costs, there are a number of other fundamental problems that limit the potential use of PCR based systems. The first among these is the inability to detect uncommon pathogens (those not on the “included” list), that may result in gross failures in cases of emerging outbreaks of one such pathogen. The second is the questionable clinical validity of some of the positive results provided by PCR based techniques. The presence of bacterial DNA in the blood may be the footprint of the transient presence of bacteria not related to any infection (Bacteria may be temporarily introduced into the blood-stream by activities ranging from surgical draining of abscesses to brushing teeth), or it may be related to the persistence of circulating DNA still detectable several days after successful anti-infectious therapy has been completed. Questions also remain regarding the suitability of the PCR based techniques to the work-flow environment in a clinic or hospital. The requirement that reagents be not only sterile (free of live bacteria), but also free of bacterial DNA requires the use of automated robotic stations for extracting DNA and performing PCR / RT-PCR analysis. This would require much larger fixed costs (for equipment) and operating costs (for high-purity chemicals). It has been suggested that fixed costs (but not necessarily operating costs of supplies) can be reduced by 4 centralizing diagnostic facilities. Centralized facilities, however, have their own drawbacks, with time lost due to transportation and queues being primary concerns in this case, where time to diagnosis is of the essence.

There also exist modern, DNA based methods for reliably typing pathogens after pure cultures have been isolated, such as Pulsed Field Gel Electrophoresis (PFGE), Multi-locus Sequence Typing and *spa* typing. But these take 48-72 hrs, require dedicated facilities and trained labor, and are low throughput. They are thus unsuitable for routine clinical practice (though used on occasions for retrospective analysis of outbreaks) (Willemse-Erix and others 2009). Ideally, any new technology that seeks to reduce the diagnosis time (either just for detection of bacterial presence and its identification, or for the previous two plus antibiotic susceptibility profiling) must not only maintain the desirable features of the current "gold standard" technologies (automated blood culture for detection, biochemical tests for identification, and disc diffusion / broth dilution for antibiotic susceptibility testing) such as clinical relevance, broad applicability (low number of false negatives), and relatively low fixed and operating costs (of ~ $20,000-30,000 and ~ $30-50 per test, respectively), but it also must be amenable to the clinical workflow. Our proposed method seeks to achieve these very goals.

1.2.4. SERS as a possible ultra-rapid alternative

Raman signals arise from inelastic scattering of light incident on a sample. The wavelength shift (energy loss) of the scattered light is characteristic of the molecular vibrations at the surface. Since only one out of 1 million photons experience Raman Scattering, traditional Raman Spectroscopy works only for bulk samples or concentrated

solutions. In 1977, Jeanmaire and van-Duyne first demonstrated a huge (over 10^6 fold) enhancement of the Raman Scattering using a roughened noble-metal as substrate. However, it has only been recently that the mechanisms leading to the surface enhancement, (electromagnetic field enhancement at “nano”- sharp edge geometries and resulting charge transfer) have been properly understood (Schatz and Van-Duyne 2002). Thus, Surface Enhanced Raman Spectroscopy (SERS) is a truly “nano” phenomena, occurring on the surface of nano-particles (Kneipp and others 2002) and on nano-textured surfaces (Moskovits 2005). When these “nano” surfaces are in contact with other molecules or materials (including cells), the scattered light conveys characteristics of the latter as well. Signal from a complex substrate (such as cell membranes) is complex, but by statistically comparing it to known signatures, one can make a good estimate about its identity.

SERS is now an increasing popular analytical method. Precisely nano-patterned substrates, specially designed for SERS, are available commercially. The Klarite™ substrates are available on a 6mm*10mm chip (with a 4mm*4mm lithographically patterned functional region). Lin has used these substrates, along with a 785 nm laser excitation line with a 10s exposure time and 30mW laser power to detect and classify spores from five *Bacillus* strains (*B. cereus* ATCC 13061, *B. cereus* ATCC 10876, *B. cereus* sp., *B. subtilis* sp., and *B. stearothermophilus* sp.), and to identify various types of vegetative bacterial cells (*Pseudomonas fragii, E. coli and Lactobacillus acidophilus*) in

food substrates (Lin and He 2008).

The main drawback of SERS at the moment is its requirement that the sample be “pure”. The proposed work will enable SERS to be applied to bacteria present in blood culture samples quickly (after < 1.5 hours of processing) as opposed to > 1 day taken by other researchers.

CHAPTER 2

KINETICALLY LIMITED DENSITY DIFFERENTIAL CENTRIFUGATION

2.1. Background

Downstream microbiological procedures, such as the desire to perform Surface Enhanced Raman Spectroscopy (SERS) as in our case, may require the user to obtain "pure" bacterial samples. This means samples in which the bacteria are present at a fairly high concentration and contain very low amounts of contaminant species (other cells, organic and inorganic inerts etc.). Since the bacteria may be present in low concentrations within complex matrices (such as soil, food, stool and blood), isolating them from these matrices is always challenging. For instance, we desire to prepare "pure" isolates of the bacteria present in positive-flagged blood culture bottles for SERS. But while these bottles contain ~10^6 bacterial Colony Forming Units (CFU)/ml of suspension, they also contain ~10^8 RBCs/ml, a smaller number of other cells (WBCs and platelets), besides proteins and other macromolecules from the growth media.

When designing the process to isolate (purify and concentrate) the target bacteria, one seeks to rely on properties that differentiate the target from other components of the matrix in which it resides. Because different matrices vary markedly in their composition, methods that work for one particular matrix may not work for another.

For instance, it is known that many bio-particles, including bacteria, have carboxyl and amino groups on their cell wall, which impart a net negative charge to them when the pH of the surrounding medium is high (>5.0). (Payne and Kroll 1991). Thus, at a high pH, they attach to positively charged surfaces, but will detach if the pH is lowered. This property of the bacteria has been leveraged to extract bacteria from soil samples using cationic ion exhange resins with an efficiency of about 35% (Jacobsen and Rasmussen 1992). However, such a method is unlikely to work for blood since there are a large number of other cells, which are also likely to adsorb and desorb along with the bacteria.

Another factor (besides selectivity of the target) that plays a major role in the choice of isolation protocol is throughput. An example of a very selective method that is not inherently high throughput is Dielectrophoresis (DEP), the motion of particles with an induced dipole in a non-uniform electric field. Their polorizability (ability to form induced dipole due to the presence of electric fields) can be used to isolate target bacteria. The DEP properties are very sensitive to cell physical and chemical properties, such as species, and has been used to separate different types of cells from each other. Herbbert and co-workers (Pohl 1978) tried to use an electrode to attract yeast in a solution, due to weak field gradients, the collection efficiency is quite low (only the yeast close to electrodes can be attracted). MEMS technology, which enables the fabrication of electrodes spaced just a few microns apart, allows the user to generate very high field

gradients (>10^6 V/m^2) and to thereby increase the collection efficiency of target particles. The main drawback of DEP is that it cannot handle large sample volumes because the high field gradients do not penetrate very far (~10-100 microns) from the surfaces of the micro-electrodes. However, as we shall describe in the next chapter, they can still be used for certain low volume “polishing” steps.

Centrifugation is perhaps the most common high-throughput method used to separate bacteria from their matrix in biology labs. Standard centrifugation is usually used to separate higher density bacterial particles from lower density matrices such as liquid growth media, milk, fruit juices etc. Differential centrifugation is a derived method based on difference in settling velocity of particles with different sizes and densities. In this method, the centrifugation speed is increased in steps. The particles with the highest density or largest size (which means highest settling velocity) will settle down fast and can then be removed from the sample. For instance, Neiderhasuer used centriguation at 100 g first to eliminate large food particles, and then to collect bacteria using a 3000g centrifugation. (Niederhauser and others 1992)

The drawback of differential centrifugation is that the centrifugation force required to pellet the larger particles (such as food debris or red blood cells in our project), is also sufficient to pellet smaller particles (such as bacteria, even though the settling velocity is less than larger particles). Consequently, contamination always exists in the

concentrated sample from the differential centrifugation method.

Density gradient centrifugation is a common method in separation with high separation efficiency. During centrifugation process, particles in the sample will migrate to the portion of the tube at equilibrium density to form a band which can be removed for future experiment. Bakken (1985) used density gradient centrifugation to separate bacterial cells from soil. However, this method requires significant density difference between the target particle and other unwanted particles, and the procedure to prepare the density gradient solution is also quite complicated. Both drawbacks limit the application of this method. In our project, the density of bacteria like *E coli* is quite close to red blood cells, which also makes this method impractical for our project.

Plate culture by itself can serve as a method to isolate bacteria from complex matrices. After some simple pretreatment methods such as centrifugation and dilution, the testing sample will spread on a growth-medium agar plate, and incubated (the growth medium may be selective or differential to a certain degree as well). The colonies formed provide a source of pure isolates of bacteria. In come cases the colony morphology itself can yield information regarding the identity of the bacteria. In most other cases, bacteria are collected from individual colonies and can be used for identification using traditional biochemical means, DNA based methods, or even by SERS. The main disadvantage of this method is, it needs a long time, usually 24 hours to get the results. But in many

cases, including ours (blood sepsis diagnosis), the need for quick results make the plate culture unacceptable (Kasai and others 2006; Mohd Adnan and Tan 2007; Balestrazzi and others 2009).

2.2. Properties of experimental material

Blood is a complex biological matrix which consists of plasma, red blood cells, white blood cells and platelets. The volume fraction of plasma to a human blood sample is about 55%. Plasma is mostly water. It also has some proteins and ions from other parts of human body. The density of plasma is quite close to water, around 1.025 g/ml. The most common type of blood cells are the Red Blood Cells (RBCs), which are also called erythrocytes. The mature human RBC are flexible biconcave disks, with a diameter of 6-8 um and thickness of 2 µm and a density of around 1.1 g/ml. The normal concentration of RBC in human body is about $4.6*10^9$/ml (Sorette and others 1991). The second most important cell type present is the White Blood Cells (WBCs), also referred to as leukocyte, from the immune system. They are slightly lighter and larger than RBCs, with densities of 1.06 to 1.08 g/ml and diameters of 10 to 12 µm. Their normal concentration is around $4*10^6$ to $1.1* 10^7$/ml (Loos and others 1976). Platelets are comparatively smaller cells whose main function is to aid in the formation of blood clots. Their size is 2 to 3 µm in diameter, their density is about 1.05 - 1.07 g/ml, and the normal concentration is $2.3*10^8$/ml (Savage and others 1986).

Bacteria, on the other hand are smaller, denser particles. For instance, Escherichia coli (*E coli*) is a gram-negative bacteria rod that is typically 2 µm long and 0.5 µm in diameter with a density of around 1.105 g/ml (Martinez-Salas and others 1981; Baldwin and Kubitschek 1984). Other bacteria also have similar densities. The density of bacteria of clinical interest has been studied in the past (primarily using equilibrium density gradient centrifugation). Invariably, the values of density reported have been relatively high. Well documented values include 1.10 g/ml for *E coli*; 1.13g/ml for *Streptococcus* (Dicker and Higgins 1987), and 1.135 g/ml for *Bacillus* (Tamir and Gilvarg 1966).

Filtered Tryptic Soy Broth (TSB) has a density approximately around 1.0 g/ml, that of plasma is 1.025 g/ml. So fluid in a suspension of 1 ml whole blood in 4 ml of TSB will have a density of 1. 005 g/ml. The density of the PBS solution is related to temperature and PBS concentration, for the room temperature (25^{o}C) and 1X PBS, the density is 1.006 g/ml (Schiel and Hage 2005). We worked with 2 kinds of mixtures: first, a mixture of sterile blood seeded with a known number of bacteria, and second, a mixture of blood, growth media, and bacteria that is similar to the contents of a blood-culture bottle by the time that it has been flagged as positive. Both of them have a fluid density between 1.0 to 1.025 g/ml.

Histopaque 1083, a commercial solution from Sigma Aldrich, is made up of polysucrose and sodium diatrizoate, and has its density adjusted to 1.083g/ml. This solution is

designed to be used to separate WBC and platelets from blood samples. However, in our project, we used it to help us to isolate bacteria, in addition to the WBCs and platelets from the RBCs (more details are presented in the following sections).

All density properties are summarized in Table 2.1.

Table 2.1 Summarized properties of experimental material

	Name	Density
Fluid	Blood plasma	1.025 g/ml
	TSB	~1.0 g/ml
	1X PBS	1.006 g/ml
	Histopaque 1083	1.083 g/ml
Particles	Red blood cells	1.1 g/ml
	White blood cells	1.06~1.08 g/ml
	Platelets	1.05~1.07 g/ml
	E coli	1.105 g/ml
	Streptococcus	1.13g/ml
	Bacillus	1.135 g/ml

2.3. Outline of the proposed technique

The process proposed to isolate bacteria from all other components of the mixture (blood cells) is shown in Figure 2.1. The process is a modified version of density differential centrifugation to isolate the target bacteria. As with density differential centrifugation, we loaded the suspension containing the target particles on top of a higher density fluid. On centrifugation, only the particles with densities higher than that of the lower denser sediment went to the bottom of the tube, whereas, those with densities lower than the dense fluid remained on top (in the original suspension, near the interface between the two fluids). The key modifications were that we ensured that the depth of the second, dense fluid (the distance through which the particles sediment) is higher than a certain critical value, and the centrifugation time is deliberately limited to a specific calculated value. Making these modifications ensures that while all of the faster settling particles (RBCs, in our case) reach the bottom, all of the slower settling ones (bacteria, in our case) remain in the lower fluid, from which they can be isolated later.

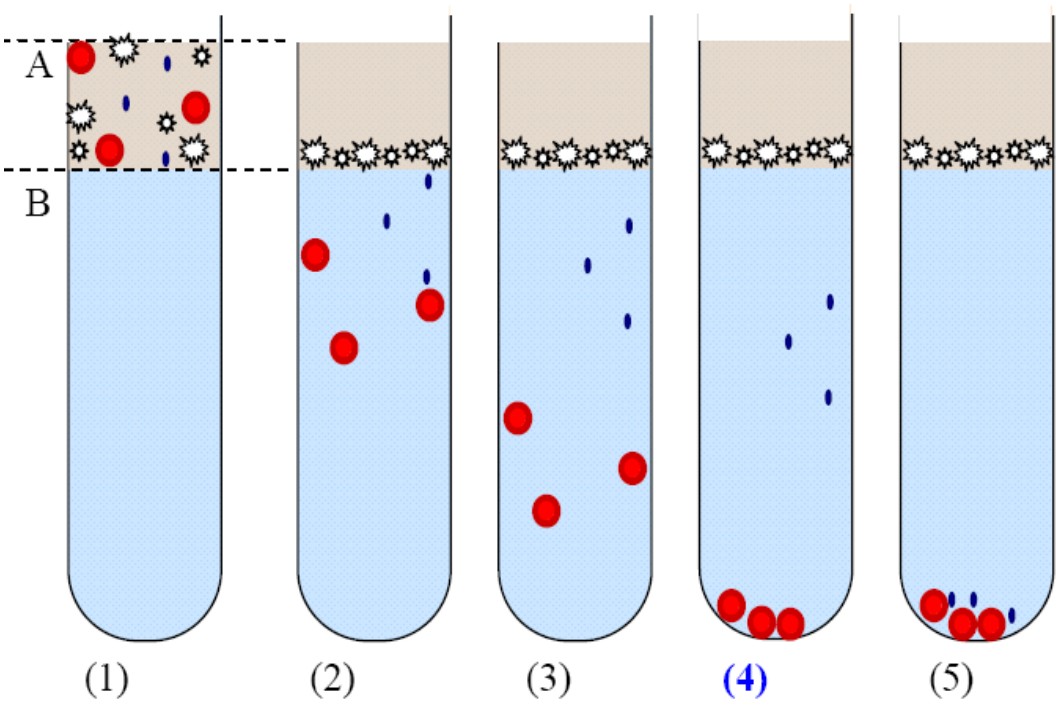

Figure 2.1 Scheme of separation process

(1): Mixture containing blood [consisting of RBCs ( ), WBCs ( ), platelets ( ) and bacteria ( )] are loaded on top of a fluid with a density less than that of RBCs and bacteria, but greater than that of WBCs and platelets. (2) Due to their density being lower than that of the lower solution, the WBCs and platelets are stopped at the interface. The RBCs and the bacteria continue the downward motion (the RBCs at a faster rate due to the larger size). (3) If the length of the lower fluid is long enough, then the RBCs that started at plane A overtake the bacteria that started at plane B, forming separate zones. (4) All the RBCs reach the bottom (form a pellet) while all of the bacteria are still in the lower solution. (5) If the process is allowed to proceed further, eventually all the bacteria reach the bottom (pellet) as well.

2.4. Experiment mathematical model

As we mentioned in the experiment outline, only *E coli* and RBC have the density greater than Histopaque 1083, thus they can pass through Histopaque and settle down. However, since the size of bacteria like *E coli* are smaller than RBCs, their settling velocity is much slower (shown in section 2.5). So, if the liquid column of Histopaque is long enough, there will be a situation where RBCs starting at Plane A (Figure 2.1) outrun bacteria starting ahead at Plane B. If we limit the time the centrifugation process runs to just the time needed for all the RBCs to settle (point 4), just a pure solution of bacteria will be left behind.

Based on the settling velocity of RBC and *E coli* in section 2.4, the required length of liquid column of Histopaque can be calculated. In order to get maximum *E coli* collecting efficiency, the time for the RBCs on Plane A to pass through both sample suspension and Histopaque 1083 need to be less than the time for *E coli* on Plane B to pass through Histopaque 1083. This can be expressed as

$$\frac{l_2}{\vartheta_{r2}} + \frac{l_1}{\vartheta_{r1}} \leq \frac{l_2}{\vartheta_{e2}} \qquad \text{Equation 2.1}$$

Which also can be transformed to

$$l_2 \geq \frac{l_1}{\vartheta_{r1}} * \frac{\vartheta_{e2}\vartheta_{r2}}{\vartheta_{r2}-\vartheta_{e2}} \qquad \text{Equation 2.2}$$

Where l2 is the length of Histopaque column, l1 is the length of sample column, ϑ_{r1} is

the velocity of RBC in sample column, ϑ_{r2} is the velocity of RBC in Histopaque, ϑ_{e2} is the velocity of *E coli* in Histopaque.

However, since we just use the solution in the Histopaque liquid column for downstream analysis, the minimum length of the Histopaque column also needs to satisfy that, when the *E coli* on Plane B to settle to the bottom, the *E coli* on Plane A need settle in the Histopaque column. This case can be expressed as

$$\frac{l_2}{\vartheta_{e2}} \geq \frac{l_1}{\vartheta_{e1}} \qquad \text{Equation 2.3}$$

Which is the same as

$$l_2 \geq \frac{l_1}{\vartheta_{e1}} \vartheta_{e2} \qquad \text{Equation 2.4}$$

Where ϑ_{e1} is the velocity of *E coli* in sample column.

From Equation 2.2 and 2.4, the length of Histopaque column l_2 needs to satisfy two minimum requirements. Therefore, in our experiment, we will calculate both their values, then use the greater one to be the minimum constrain.

The best time to collect *E coli* is when all RBCs settle down to the bottom, while most of *E coli* are left behind in Histopaque. In other words, the collection time is after settling down time of RBC, and before the settling down time of *E coli*.

The settling down time of RBC is given by

$$t_{RBC} = \frac{l_1}{\vartheta_{r1}} + \frac{l_2}{\vartheta_{r2}} \qquad \text{Equation 2.5}$$

Similarly, the settling down time of *E coli* is

$$t_{ecoli} = \frac{l_1}{\vartheta_{e1}} + \frac{l_2}{\vartheta_{e2}} \qquad \text{Equation 2.6}$$

The number of *E coli* and RBC profiles in the Histopaque liquid (layer 2) are shown in Figure 2.2, the pink box is the appropriate time range for collecting *E coli*. The starting time is the settling time of RBC, and the stop time is the settling time of E coli. In that time range, we can collect most of the *E coli* and eliminate other unwanted bio-particles (RBCs, WBCs and platelets).

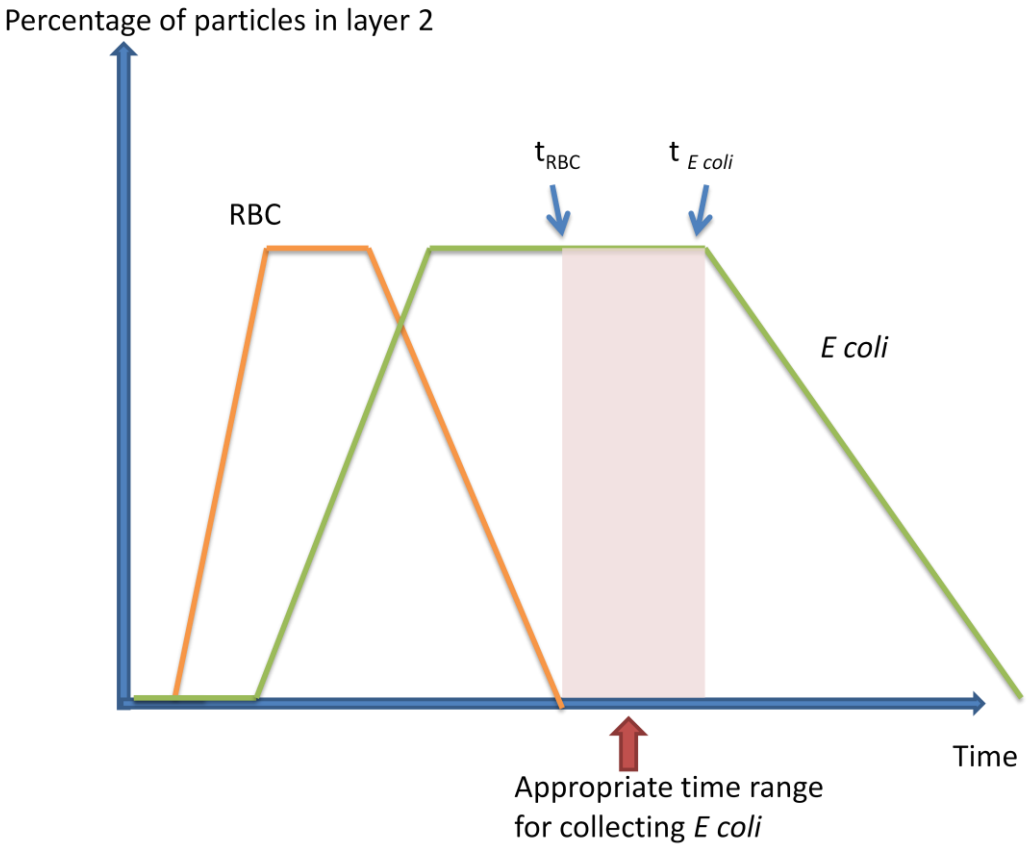

Figure 2.2 Percentage changes of RBC and *E coli* in layer 2 at different times

2.5. Calculating sedimentation velocities in our system

2.5.1. Sedimentation of individual particles

When a particle happens to be denser than the liquid in which it is suspended, it experiences a net force downward that is the difference between its weight and its buoyancy. For a spherical particle of density ρ and radius R suspended in a liquid of density ρ_l, this force is given by

$$G = \frac{4}{3}\pi R^3 \Delta\rho g \qquad \text{Equation 2.5}$$

$\Delta\rho$ is the density difference between particle and surrounding medium.

This force is counteracted by the viscous drag of the fluid. For a spherical particle moving though a continuous Newtonian fluid at low to moderate velocities (Reynolds Numbers < 1) the drag force is given by the Stokes Equation (Equation 2.6)

$$F = 6\pi\mu R\vartheta \qquad \text{Equation 2.6}$$

where, μ is the fluid's viscosity

R is the radius of the spherical object

ϑ is the particle's velocity

The particles settle (move downwards) with a velocity for which the two forces are

balanced. This velocity, obtained by equating equations 2.1 and 2.2 is thus given by

$$\vartheta = \frac{2\Delta\rho}{9\mu} R^2 g \qquad \text{Equation 2.7}$$

Stokes' law applies when the Reynolds number, Re, of the particle is less than 0.1. For the experiment in our project, the Re was less than 10^{-4}. In our experiment, the centrifugation speed was 400g, viscosity of all the fluids are 0.001 kg/(m·s).

The basic concept is applicable to particles of other shapes as well. But in these cases, Equation 2.3 needs to be modified, and an "effective radius" used for R. The effective radius can be calculated analytically for certain geometries. For instance, for a prolate spheroid (a spheroid for which the polar axis is greater than the equatorial diameter, like American Football), the effective radius is given by

$$R = \frac{\sqrt{a^2 - b^2}}{\ln\left(\frac{a+\sqrt{a^2-b^2}}{b}\right)} \qquad \text{Equation 2.8}$$

where, a is the major axis radius, b is the minor axis radius. On the other hand, for an oblate spheroid (an ellipsoid with a polar axis shorter than the equatorial diameter, like M&M candies), the effective radius is given by

$$R = \frac{\sqrt{a^2 - b^2}}{\tan^{-1}\left(\sqrt{\frac{a^2-b^2}{b^2}}\right)} \qquad \text{Equation 2.9}$$

In our case, we modeled "rod" shaped *E coli* bacteria as prolate speroids with a major axis of 1 µm, and a minor axis of 0.5 µm, and RBCs as oblate spheroids with a major axis of 3.5µm and a minor axis of 1µm. Consequently, supposing the centrifuge velocity is

400 rcf, we predicted sedimentation velocities of $2.67*10^{-5}$ m/s and $6.56*10^{-6}$ m/s for *E coli* though layer 1 (consisting of plasma and PBS) and layer 2 (high density Histopaque solution), respectively. The corresponding values for RBCs are $5.01*10^{-4}$ m/s and $1.01*10^{-4}$ m/s.

2.5.2. Hindered settling

For a single spherical particle settling in an infinite fluid, we can use Stokes law to describe the behavior. If there are some interactions of particles in the fluid or the interactions of the particles with the container walls, the settling behavior will be modified (usually retarded). Settling that is significantly modified in such a manner known as hindered settling. A number of semi-analytic or empirical expressions are available to calculate effective settling velocities for systems with hindered settling. (Felice and Kehlenbeck 2000)

One such correlation is the Richardson-Zaki Correlation, where the effective settling velocity is given by

$$\vartheta' = \vartheta G(\emptyset) \qquad \text{Equation 2.10}$$

where

$$G(\emptyset) = (1 - \emptyset)^{4.7} \qquad \text{Equation 2.11}$$

($\emptyset$ being the volume fraction number of all particles). For our project, in the first mixture (sterile blood seeded with a known number of bacteria, diluted by PBS as 1:1),

the volume fraction of red blood cells was about 0.25, given the volume fraction of RBC in whole blood was about 50%. In the second mixture of blood, growth media, and bacteria, the volume fraction of red blood cells was 0.1 (supposing the ratio of blood to growth media is 1:4).

Therefore, when taking hindered effect into consideration, supposing the centrifuge velocity is 400 rcf, in the first mixture, the velocities of RBC though layer 1 (consisting of plasma and PBS) and layer 2 (high density Histopaque solution) are $1.30*10^{-4}$ m/s, $2.62*10^{-5}$ m/s respectively. In the second mixture, the velocities are $3.07*10^{-4}$ m/s, $6.18*10^{-5}$ m/s respectively.

2.5.3. Cluster sedimentation

In some cases, particles undergoing sedimentation may aggregate and form clusters during the process. As effectively larger "particles" are formed by the aggregation of smaller ones, the process of sedimentation speeds up. We observed such an effect (collection of aggregated particles) for RBCs in Histopaque 1083 (but importantly, not for *E coli*). Cluster sedimentation was studied by Allain. (Allain and others 1996) They assumed the cluster behaves as an impenetrable sphere with a hydrodynamic radius R_H, and the velocity of the cluster can be expressed as

$$\vartheta = \frac{2\Delta\rho a^2}{9\mu}\frac{a}{R_H}gs \qquad \text{Equation 2.12}$$

where a is the radius of the individual particle, s is the number of particles in an

aggregate, and will scale with R as s~(R_H /a)^D, where D is the experiential number (from their experiment they find D is about 2.2). Therefore, the settling velocity of the cluster now becomes

$$\vartheta = \vartheta_0 \left(\frac{R_H}{a}\right)^{D-1} \qquad \text{Equation 2.13}$$

where ϑ_0 means the settling velocity of the individual isolated particle. From our observations, there will be approximately 100 RBCs in each cluster, thus, taking into account both clustering and hindered settling, the settling velocities of RBC in the Histopaque layer are predicted to be around 1.39*10^{-4} m/s.

All the velocity calculating results are summarize in Table 2.2 (supposing centrifugation speed is 400 rcf)

Table 2.2 Summarized calculating velocity results

Particle	Solution	In what condition	Velocity Result
E coli	Sample suspension	Normal	$2.67*10^{-5}$ m/s
	Histopaque 1083	Normal	$6.56*10^{-6}$ m/s
RBC	Sample suspension	Normal	$5.01*10^{-4}$ m/s
	Histopaque 1083	Normal	$1.01*10^{-4}$ m/s
	Sample suspension	Hindered effect	$1.30*10^{-4}$ m/s
	Histopaque 1083	Hindered effect	$2.62*10^{-5}$ m/s
	Histopaque 1083	Cluster sedimentation (s=100)	$1.39*10^{-4}$ m/s (D=2.1)
			$1.89*10^{-4}$ m/s (D=2.3)
			$2.56*10^{-4}$ m/s (D=2.5)
			$3.47*10^{-4}$ m/s (D=2.9)

2.6. Experiment design and procedures

Following the protocol for Histopaque 1083, the volume for suspension (blood sample) is 3 ml, which will translate to a 3 cm length of liquid column in an Eppendorf centrifuge tube. The volume of Histopaque 1083 is the same, but the length will be slightly greater than 3 cm because of the cone end of the tube. From previous data, the lengths of both liquid columns meet the requirements as specified earlier in the section on modeling.

Given 3 cm of both sthe ample and Histopaque column, from Equations 2.3 and 2.4, as well as velocity results in section 2.5, the time for all RBC to settle down is about 15 min, whereas for *E coli* is about 80 min. That is to say, when all RBC get settle down, most of *E coli* are still in Histopaque 1083 layer.

Based on the mathematical model and calculations in previous sections, we conducted the following experiment to verify our method.

The experiment procedure is listed as follows:

1. Sample preparation.

For the first mixture, the blood sample is sterile swine blood, and then seeded with 10^6 CFU/ml *E coli*.

The second mixture is blood culture. Sterile swine blood is diluted by TSB at a 1:4 ratio, then seeded with 10^2 CFU/ml *E coli*. The mixture is incubated for about 12 hours to let the *E coli* grow to 10^6 CFU/ml.

2. Centrifugation procedures.

Following the protocol of Histopaque 1083, 3.0 ml Histopaque 1083 is added to the centrifuge tube, and then 3.0 ml blood mixture is carefully loaded onto the Histopaque 1083 surface, then centrifuge at 400 rcf (400 g) for different times at room temperature. After centrifugation, the plasma/PBS suspension layer, Histopaque 1083 layer, and the RBC sedimentation layer are carefully transferred into different EP tubes, for future plate counting and RBC cell counting.

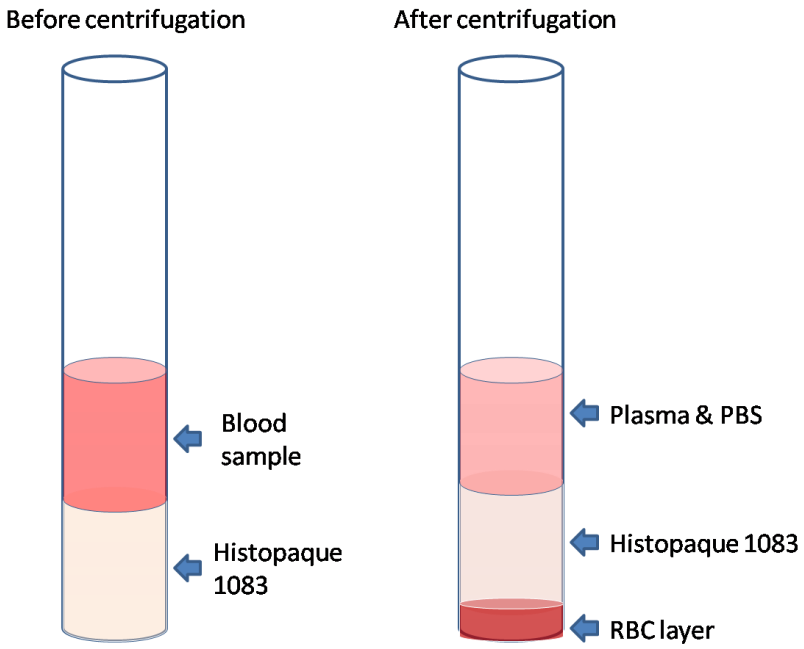

Figure 2.3 Scheme of centrifugation experiment

3. Counting procedures.

Classic plate counting method is used for *E coli* counting. Each sample has 3 individual plates for counting the colony, and then the average number was taken for the final

results.

For RBC, when the concentration is greater than 10^6 /ml, it was counted using hemocytometer. Otherwise, when the concentration is less than 10^6 /ml, the sample was first mixed with RBC lysis buffer, then the absorbance spectrum of lysis sample was measured.

2.7. Experiment data and discussion

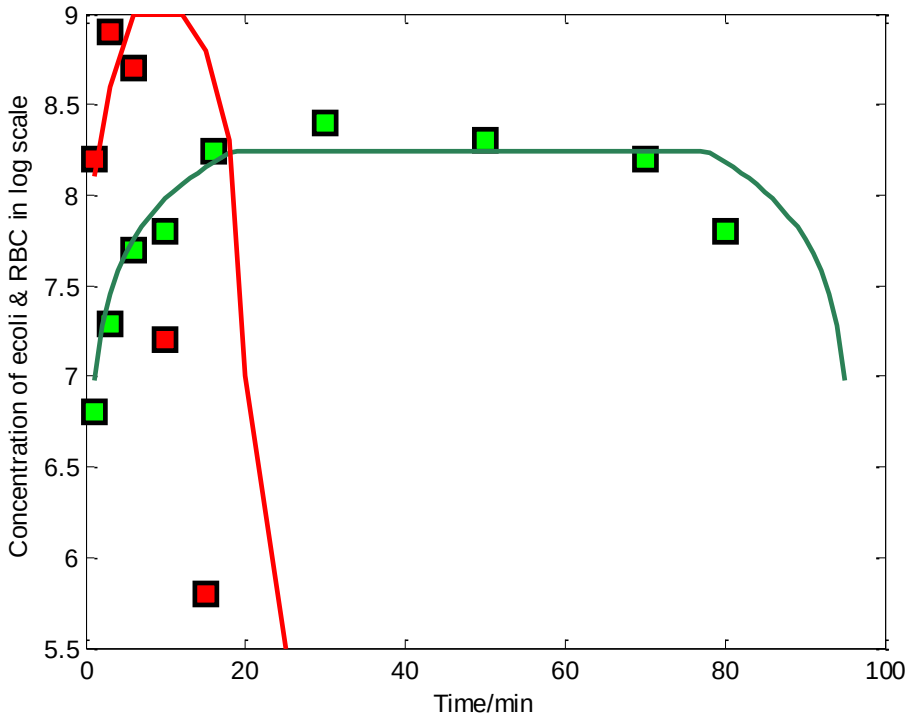

Figure 2.4 Observation and prediction concentrations of *E coli* /RBC in Histopaque 1083 layer at different time.
The red squares are observation number of RBC in log scale, and the red line is the prediction number; the green squares are observation number of *E coli*, while green line is the prediction. Each observation data point is the average number of three individual experiments data.

Both prediction concentrations of *E coli* and RBC were calculated using the following equation

$$C_{His} = \frac{C_{initial}\,\delta t}{L_{His}} \qquad \text{Equation 2.14}$$

where L_{His} is the length of the Histopaque 1083 layer in the centrifuge tube. The

velocities of RBC and *E coli* are from section 2.5.

For red blood cells, the ascending rate of observation is quite close to prediction, while the descending rate of observation is much less. That is because polysucrose, the ingredient of Histopaque, will aggregate red blood cells to form clusters, which will greatly increase the settling velocity, according to section 2.5. The RBC clusters usually consist od hundreds of cells, so as to increase the settling velocity by 20~100 times, compared to isolated individual cells. In that case, when blood cells pass through the interface of Histopaque 1083, most of them will form clusters and settle down in less than 2 minutes.

For *E coli*, the concentration change of observation is quite similar to prediction, despite a bit different in the descending part. The reasons to cause such difference should be: a) the density of *E coli* in our experiment was not exactly 1.10 g/ml, some of them were slightly denser, which makes them move much faster in Histopaque 1083 than other *E coli*; b) there can be some errors in plate counting, which will affect the observation concentration; c) some *E coli* can aggregate together in solution, then slightly increase their settling velocity.

Although there are some differences between observation and prediction, we can still see the significant distinction in settling velocities. As we predicted in Figure 2.2 and

Figure 2.3, after some minutes in centrifugation, almost all blood cells settled down while most of the *E coli* will keep in the Histopaque 1083 layer. From the experiment's results, 40 to 60 minutes after starting will be the best time to isolate *E coli*. Since the density doesn't vary too much in different bacteria species, we believe our method will also be applicable to other bacteria such as *Streptococcus, Bacillus* and so on.

The bacteria enriched solution was used in following experiment, Flow Through Dielectrophoresis.

CHAPTER 3

DIELECTROPHORESIS (DEP)

3.1. Introduction to DEP

Electric fields can induce the formation of dipoles even in particles that have no net charge. In a non-uniform electric field, a particle with such an induced dipole will experience a net force from the surrounding electric field. The migration of the particle caused by electric net force is termed as dielectrophoresis (DEP). The DEP force on an isotropic, homogeneous dielectric spherical particle is expressed as

$$F_{DEP} = 2\pi\varepsilon_0\varepsilon_m r^3 \mathrm{Re}(f_{cm})\nabla {E_{rms}}^2 \qquad \text{(Equation 3.1)}$$

where ε_0 is the permittivity of free space, ε_m is the relative permittivity of surrounding medium, r is radius of particle, E_{rms} is root mean square electric field around the particle, and $\mathrm{Re}(f_{cm})$ is the real part of Clausius-Mossotti (CM) factor, which can be expressed as

$$\mathrm{Re}(f_{cm}) = \mathrm{Re}\left(\frac{\varepsilon_p^* - \varepsilon_m^*}{\varepsilon_p^* + 2\varepsilon_m^*}\right) = \frac{(\varepsilon_p - \varepsilon_m)*(\varepsilon_p + 2*\varepsilon_m) + \frac{1}{\omega^2}*(\sigma_p + 2*\sigma_m)*(\sigma_p - \sigma_m)}{(\varepsilon_p + 2*\varepsilon_m)^2 + \frac{1}{\omega^2}*(\sigma_p + 2*\sigma_m)^2} \qquad \text{(Equation 3.2)}$$

where ε_p^* and ε_m^* are complex permittivity ($\varepsilon^* = \varepsilon - \frac{i\sigma}{\omega}, i = \sqrt{-1}$) of particle and

medium, respectively (σ_p and σ_m are the respective conductivities). (Chen and others 2007)

It can also be seen that for high frequencies (w → infinity), the CM factor reduces to

$$\mathrm{Re}(f_{cm}) = \frac{(\varepsilon_p - \varepsilon_m)}{(\varepsilon_p + 2*\varepsilon_m)} \qquad \text{(Equation 3.3)}$$

whereas for low frequencies (w → 0), it reduces to

$$\mathrm{Re}(f_{cm}) = \frac{(\sigma_p - \sigma_m)}{(\sigma_p + 2*\sigma_m)} \qquad \text{(Equation 3.4)}$$

Thus, at high frequencies, the CM factor is proportional to differences in the permittivities of the particle and the medium, whereas at low frequencies, it is proportional to differences in their conductivities. Further, it may be noted that the CM factor can be positive or negative. When it is positive, the DEP force is directed towards regions of high electric field strength, whereas when the CM factor is negative, the DEP force is directed towards regions of low electric field strength. Thus, a polizable particle can either move towards regions of high electric field strength (positive DEP or pDEP), or regions of low electric field strength (negative DEP or nDEP), depending on (a) the permittivity of the particle, (b) the conductivity of the particle, (c) the permittivity of the medium (d) the conductivity of the medium, and (e) the frequency of the applied field, if it happens to be alternating (AC).

A salient feature of DEP is that the same particle can display p-DEP behavior at a

particular range of frequencies and n-DEP behavior over a different range. This typically happens if the conductivity of the particle is greater than the surrounding medium, but its dielectric constant (permittivity) is lower (or vice-versa). In such a scenario, the particle will display p-DEP at low frequencies, and n-DEP at high frequencies (the reverse being true for the vice-versa case), and there will also exist a critical frequency, called cross-over frequency (COF) given by

$$\omega_{COF} = \sqrt{\frac{(\sigma_p + 2*\sigma_m)*(\sigma_m - \sigma_p)}{(\varepsilon_p - \varepsilon_m)\,(\varepsilon_p + 2*\varepsilon_m)}} \qquad \text{(Equation 3.5)}$$

If different types of particles have different conductivities and/or permittivities, then they will have different COFs when dispersed in the same medium. Hence, at selected frequencies, (such as at a frequency higher than the COF of one particle, but lower than that of the other), one particle type may experience p-DEP, and the other n-DEP, thus providing a means of separating them. (Cheng and others 2007)

3.2. DEP behavior of bio-particles

Of special interest to us is the DEP behavior of biological particles such as bacteria of various species and blood cells of various types. Figure 3.1 shows the typical DEP behavior of biological cells when placed in a low conductivity buffer (σ < ~ 100 µS/cm).

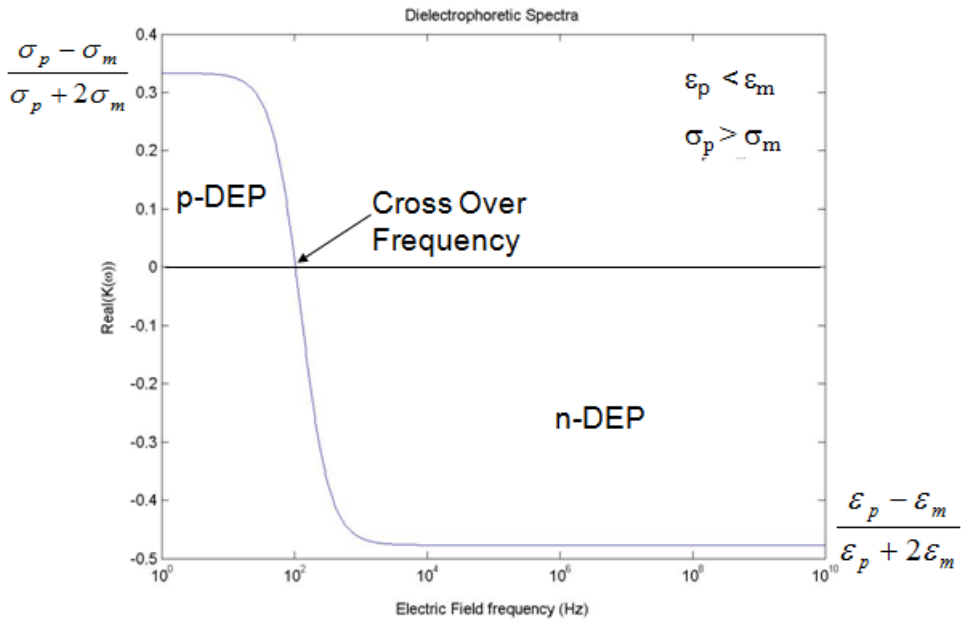

Figure 3.1 Scheme of dielectrophoretic spectra

That we are able to observe DEP behavior in bio-particles implies that an effective dipole is formed within the particle, that is then pulled by net force in the non-uniform electric field. A number of sources contribute to determine the net effective polarizability of bio-particles. A very important one is the cell membrane, which, while made up primarily of a phospholipids bilayer, also harbor numerous protein and sugar molecules that serve as capacitative regions and produce charge distributions. Different species, which have characteristically different proteins and membrane composition, can hence be expected to show differences in DEP behavior. Also contributing to the effective polarizability is the cytoplasm, that contains molecules like DNA, RNA, proteins, etc. that are polarizable, but whose relative proportions may not vary as markedly among different species (Pohl 1978).

3.3. COF measurement of *E coli,* and Red Blood Cells

We experimentally studied the DEP behavior of two bio-particles of particular interest to us: *E coli* (a representative bacterium) and Red Blood Cells (RBCs). Our experimental process is described below

3.3.1. Quadruple electrodes

As mentioned earlier, different bioparticles always have much different DEP effects in the same electric field. Before we use such difference in future experiments (like sorting), the exact DEP properties need to be measured. Generally, cross-over frequency (COF) will be used as the parameter to characterize the DEP behavior of a particular type of bio-particle.

The quadruple electrodes were used in the COF experiment. Each set of electrodes consisted of four symmetric gold electrodes. The gap distance between electrodes was about 20μm and the thickness of gold layer was 100nm. They were fabricated using a process described in Section 4.4.

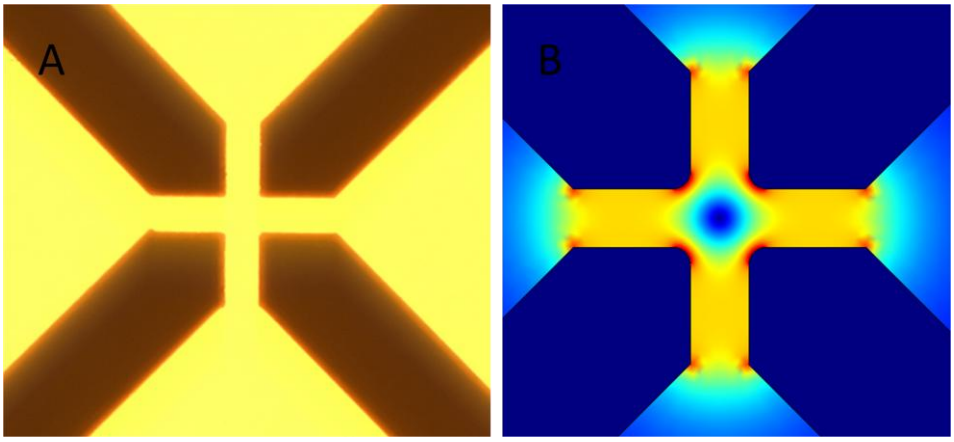

Figure 3.2 Quadruple electrodes
(A) (Left) photo of quadruple electrodes. (B) (Right) Finite element simulation (using COMSOL) of electric field distribution produced by quadruple electrodes

The AC signal from signal generator was applied to the electrode during the experiment. The left-top and right-bottom electrodes connected to the “live” port, while the rest two electrodes connected to the “neutral” port. After applying voltage, the high local electric field was generated between electrodes. From the finite element method result in Figure 3.2B, the regions between electrodes had the highest local intensity, and the symmetric center had the lowest (in the simulation, the dark blue dot in the center of the figure represents the lowest electric field intensity). Consequently, if the particle experiences positive DEP mobility, it will move to the region between the electrodes, and if it experiences negative DEP the particle will move toward the center.

Since the solution in which the particles are suspended has a large effect on the behavior of the bio-particles, we must first sediment out the particle from whichever solution it happens to be in (plasma, growth media etc) and resuspend in our buffer of

choice (e.g. 1X manitol + saline + amino-hexanoic acid (AHA)) This “centrifugation and resuspension step” may need to be repeated 2 to 3 times to ensure that the properties of the suspending solution are as desired. Electrodes are connected to the signal generator while the output is kept in the off state. The output voltage is set to 6 Vp-p, and the initial frequency to 100 kHz. The motion of particles will be recorded (usually be positive-DEP at this frequency, which means move toward the gap between electrodes). The frequency is tuned higher step wisely until the particles suffer negative-DEP, which means move toward center. The frequency when particles turn to be negative-DEP is the cross-over frequency. Procedure 4 requires repeating several times until a stable result is accomplished.

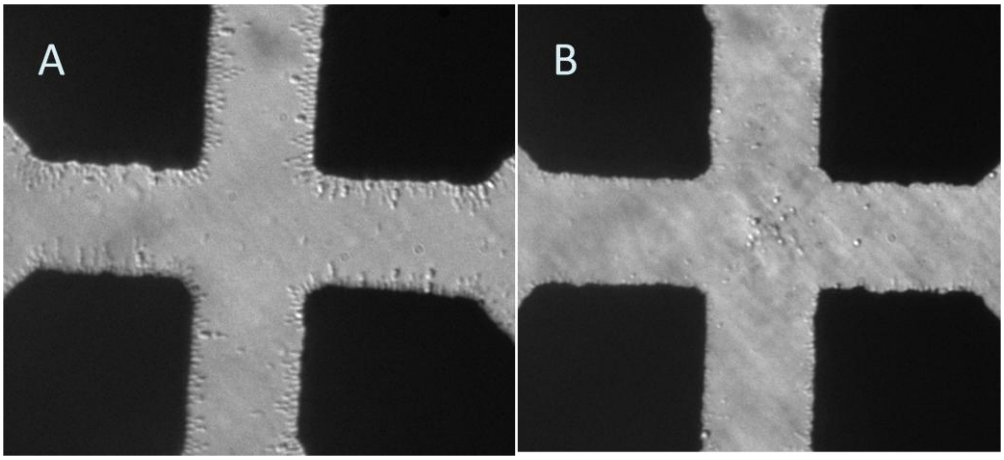

Figure 3.3 Photos of particles with different DEP properties
A, photo of particles that have positive DEP;
B, photo of particles that have negative DEP

3.3.2. COF measurement result (*E coli* and RBC in different solutions)

There are practical limitations on the frequency range that we can test, and on the frequencies that can be used when carrying out the sorting in future. The available signal generator can only produce a signal with frequency up to 120 MHz. Also, at low frequencies (< 100 KHz) bubbles are generated due to electrolysis. Hence, it would be ideal if the cross-over frequencies for different cell types were not only distinct, but also were within this range (100 KHz to 120 MHz). One way to achieve these goals is to modulate the conductivity and permittivity of the solution that the particles are suspended in. As seen in Equation 3.5, changing the solution conductivity (σ_m) and permittivity (ε_m) will change the COF of the particle. Our basic solution is an isotonic solution of Mannitol. Mannitol is a sugar-alcohol that most bacteria are not able to metabolize. Hence, the bacteria remain in a static (non-growth) phase during the time they are suspended in the solution. Mannitol also happens to not affect the conductivity or the permittivity of the solution in a measurable manner. We adjusted the conductivity of the solution by adding known amounts of saline (NaCl solution) and the permittivity by adding known amounts of Amino-Hexanoic Acid (AHA). AHA is a qwitterionic molecule that has both positive and negative charged groups, and hence contributes significantly to the permittivity of the solution, while only weakly affecting the conductivity. As reported in Table 3.1, a solution consisting of a mixture of Mannitol, saline (NaCl) and AHA was found to ensure that the COF of the bacteria and RBCs were

as desired.

The COF of *E coli* and RBC in different DEP solutions are summarized in the Table 3.1.

Table 3.1 COF of Red blood cells in mannitol mixture

Basic solution 1X mannitol	No NaCl	0.02% NaCl
No AHA	All + in 100kHz~120MHz	
0.4M AHA	23 MHz from + to -, weak mobility in (20~28 MHz)	30 MHz from + to -, weak mobility in (20~30 MHz)
1M AHA	8 MHz from + to -, weak mobility in (5~20 MHz)	10 MHz from + to -, weak mobility in (5~15 MHz)

Table 3.2 COF of *E coli* in Mannitol mixture

Basic solution 1X mannitol	No NaCl	0.02% NaCl
No AHA	All + in 100kHz~120MHz	
0.4M AHA	60 MHz from + to -, weak mobility in (20~100 MHz)	75 MHz from + to -, weak mobility in (30~90 MHz)
1M AHA	22 MHz from + to -, weak mobility in (20~80 MHz)	60 MHz from + to -, weak mobility in (50~75 MHz)

In order to utilize the DEP difference to isolate *E coli* from bacteria, we used a solution that could provide a significant difference between target particles. As shown in Table 3.1 and 3.2, 1X mannitol + 1M AHA + 0.02% NaCl was the choice. The principle to separate *E coli* or other bacteria from blood cells using our device was discussed in the next chapter.

3.3.3. Measurement of dielectrophoretic mobility

A more rigorous way to examine the DEP behavior of bioparticles is to obtain the dielectrophoretic mobility of the bio-particle at various frequencies. The DEP force that a particle suspended in solution experiences is balanced by the drag on the particle, and the particle moves with a constant velocity.

From the previous chapter, the stokes drag force for sphere particle is $F = 6\pi\mu r\vartheta$, which will balance the force from DEP shown in Equation 3.1. In this case, $F = 6\pi\mu r\vartheta = 2\pi\varepsilon_0\varepsilon_m r^3 \mathrm{Re}(f_{cm})\nabla {E_{rms}}^2$. Consequently, we get

$$\vartheta_{DEP} = \frac{r^2}{3\mu}\varepsilon_m Re(f_{CM})\ \nabla {E_{rms}}^2 \qquad \text{(Equation 3.6)}$$

r, radius of the particle; μ, viscosity,

The definition equation of DEP mobility is given by

$$\vartheta_{DEP} = -\mu_{DEP} * \nabla E_{rms}^2 \qquad \text{(Equation 3.7)}$$

Where ϑ_{DEP} is the velocity; μ_{DEP} is DEP mobility

∇E_{rms}^2 is the gradient of E_{rms}^2, which can be expressed as

$$\nabla E_{rms}^2 = \nabla\left(E_x^2 + E_y^2\right) = \left[2 * E_x * \frac{\partial E_x}{\partial x} + 2 * E_y * \frac{\partial E_y}{\partial x}, 2 * E_y * \frac{\partial E_y}{\partial y} + 2 * E_x * \frac{\partial E_x}{\partial y}\right]$$

(Equation 3.8)

For a spherical particle,

$$\mu_{DEP} = -\frac{r^2}{3\mu}\varepsilon_m Re(f_{CM}) \qquad \text{(Equation 3.9)}$$

$Re(f_{CM})$, real part of the Clausius-Mossotti factor

3.3.4. Mobility calculation procedures

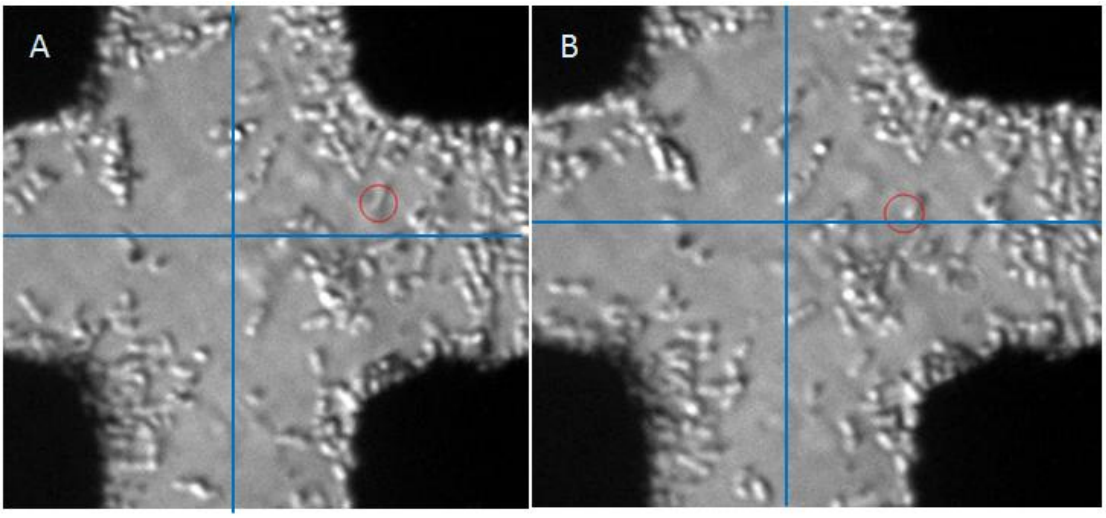

Figure 3.4 Some frames of moving pseudomonas used in mobility calculation.

1. The video of moving target particles is recorded (by *Q-Capture*) when particles suffer either p-DEP or n-DEP force. Then it is opened in *Image J* to generate several frames showing the moving process of particles.

2. The center of quadruple electrodes is located will be set as the origin point of coordinate axes. The proper particle is selected which has clear motion and the direction doesn't change too much during the whole moving process, shown in the red circle in Figure3.4. Then get the normalized coordinates of the particles mass center in each frame, given that the distance of gap between electrodes is 20μm. For example, the normalized coordinates of a particle in Figure 3.4A are [11.2 2.8]; in Figure 3.4B are [10.1 1.0] (Unit is μm).

3. Given the time interval between each frame in the video is 0.328 sec, and the normalized coordinates of the particle in each frame, the average velocity can be calculated between those frames. The average velocity from Figure 3.4A to Figure 3.4B is: [-3.35 -5.49] ((x2-x1)/0.328, (y2-y1)/0.328, unit is μm /s);

4. According to Equation 3.7, the mobility is velocity divided by ∇E_{rms}^2. In order to get more accurate result, the ∇E_{rms}^2 calculated in the center point of the moving process will be used in calculation. The gradient result can be calculated in COMSOL using Equation 3.8.

For instance, the center point from Figure 3.4A to Figure 3.4B is [10.65 1.9];

From COMSOL, the value of ∇E_{rms}^2 at [10.65 1.9] is [3.10e15 1.03e15] (unit is V^2/m^3)

According to Equation 3.3, $\mu_{DEP} = -\frac{v_{DEP}}{\nabla E^2} \approx -\frac{|v_{DEP}|}{|\nabla E^2|}$, so μ_{DEP} is -1.97*10^{-21} (unit is V^2/m^4)

5. Procedures 1 to 4 will be repeated for each frame, as well as for each video (usually have some different videos for the same particle), to get average mobility for the particle. For instance, according to our calculation, the average mobility of *pseudomonas* in 1MHz is -2.10*10^{-21} V^2/m^4

CHAPTER 4

MEMS DEVICE DESIGN AND FABRICATION

4.1. DEP behavior of bio-particles in device

The Purpose of our device is to be able to sort particles at high throughput (> 100 particles/sec). The combination of laminar fluid flow and DEP will help us to realize our goal. As shown in Figure 4.1A, when the electric field is absent, all particles in fluid flow will keep the same direction of motion, which is the same as the streamline of fluid flow (supposing the flow is laminar, which will be discussed more in section 4.3).

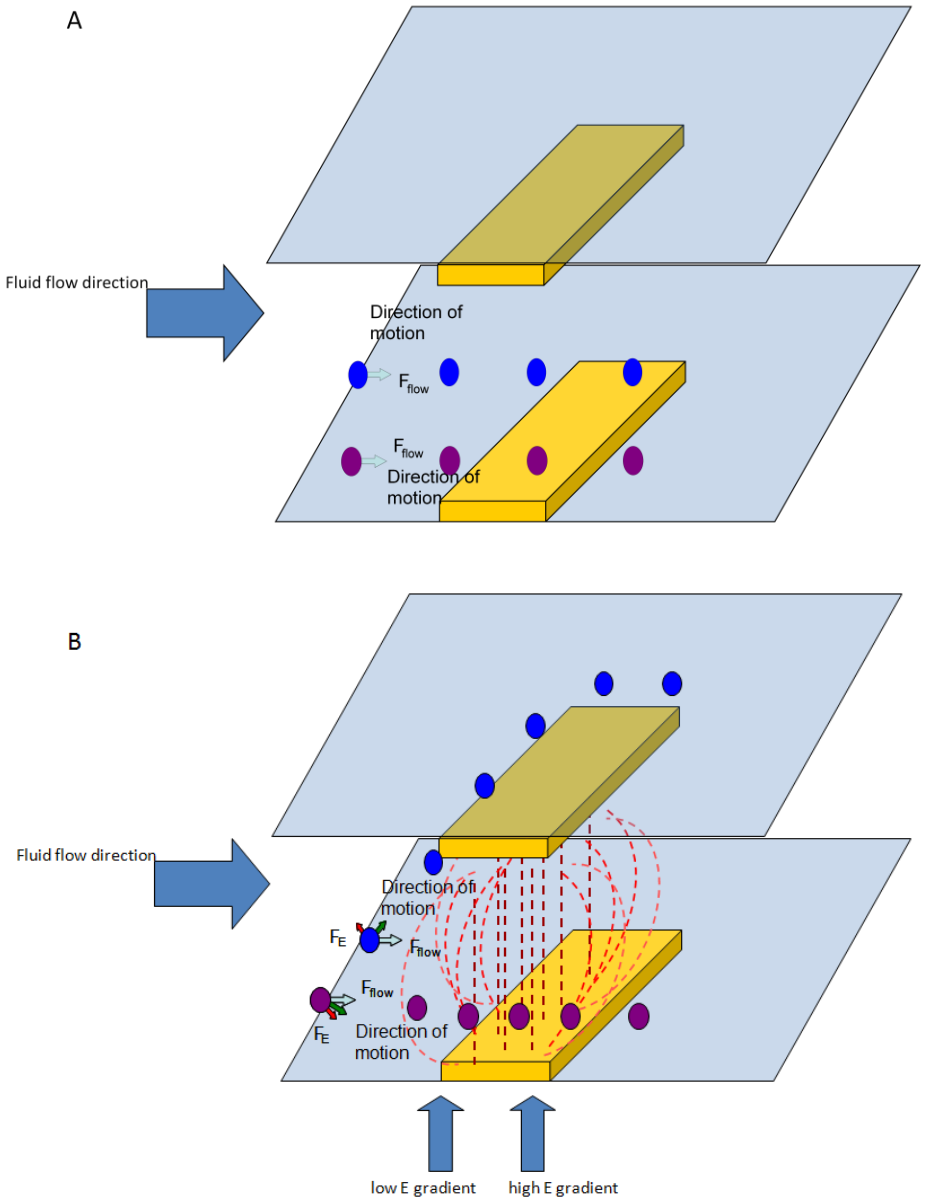

Figure 4.1 Scheme of bio-particles behavior in device.
The purple dot is positive-DEP bio-particle and blue dot is negative-DEP bio-particle.

As shown in Figure 4.1B, a particle experiencing p-DEP (purple dot) will suffer a DEP

force (red arrow) directed towards regions of the high electric field (the gap space between the parallel electrodes in this figure). At the same time, moving fluid will also apply a force (light blue arrow) on the particle. Finally, if we ignore the gravity (usually very small for bio-particles in solution), the direction of the composition force (green arrow) will be toward the electrodes. The combined effect of the two forces causes the particle to be drawn into the region between the electrodes and remain at, or very near, its original streamline. On the other hand, if the particle experiences n-DEP (blue dot), the DEP force will act in the opposite direction, trying to repel the particle from the region between the electrodes. The fluid force, however, continues to act in the same direction. Therefore, the direction of the effective force will be parallel to electrodes. The n-DEP bio-particles will traverse a path parallel to the electrodes, and once the electrode ends, will begin flowing along the local streamline of the fluid.

4.2. Device design

In order to validate the core sorting technology that works based on a combination of AC electric fields and laminar microfluidic flow, we fabricated and tested an integrated microfluidic chip to separate target bio-particles (bacteria and RBC). Bio-particles suffer the DEP force from the electric field generated by electrodes in the device, and then have different moving behaviors, either attracted or repelled by electrodes, based on their different DEP properties. This device is very similar to that used by Cheng and

others (2007).

4.2.1. Outline of 1st generation device function

This first generation integrated chip, shown in Figure 4.2, involves four different stages: trapping, focusing, sorting, and collecting.

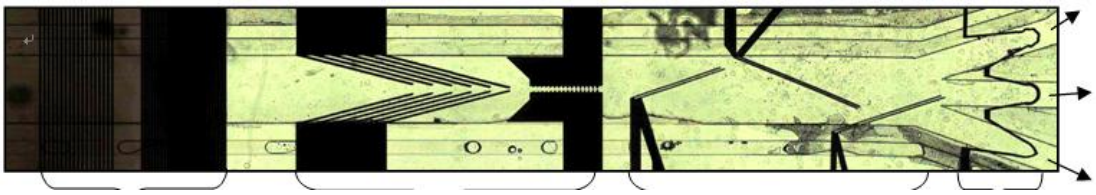

Figure 4.2 Photo of the 1st generation device (Cheng and others 2007)

The first parallel planar electrode array from the inlet (the left-most part of Figure 4.2) is called the trap. The design of the trap is such that it captures all particles that suffer positive DEP while allowing those that suffer from negative DEP to pass through. This trap is operated at a low frequency, and unwanted debris which displays positive DEP can be trapped by this structure. As will be explained in the next section (future work), this selectivity can, and if needed, be employed to enhance the capabilities of the 2nd generation sorter.

The second stage of the device is the “focusing unit.” It has two parts, which have different types of planar electrodes. Both these electrodes are operated at a relatively high frequency. At this frequency, all the particles (RBC and Bacteria) suffer negative DEP,

and are repelled by electrodes then hence directed toward the center of the channel. The first pair is a coarser focusing unit, bringing the particles from the entire 1mm channel to a width of 50 µm, while the second set of electrodes (the interdigitated ones) are used for a finer focusing process, bringing the particles to a region of 20 µm and forming a single line of particles. Bringing all the particles into single file along the center of the channel ensures that when they reach the sorter downstream, all the particles will experience the same fluid flow field and electric field, and hence their behavior in the sorter will be determined solely by the dielectrophoretic properties of the particles.

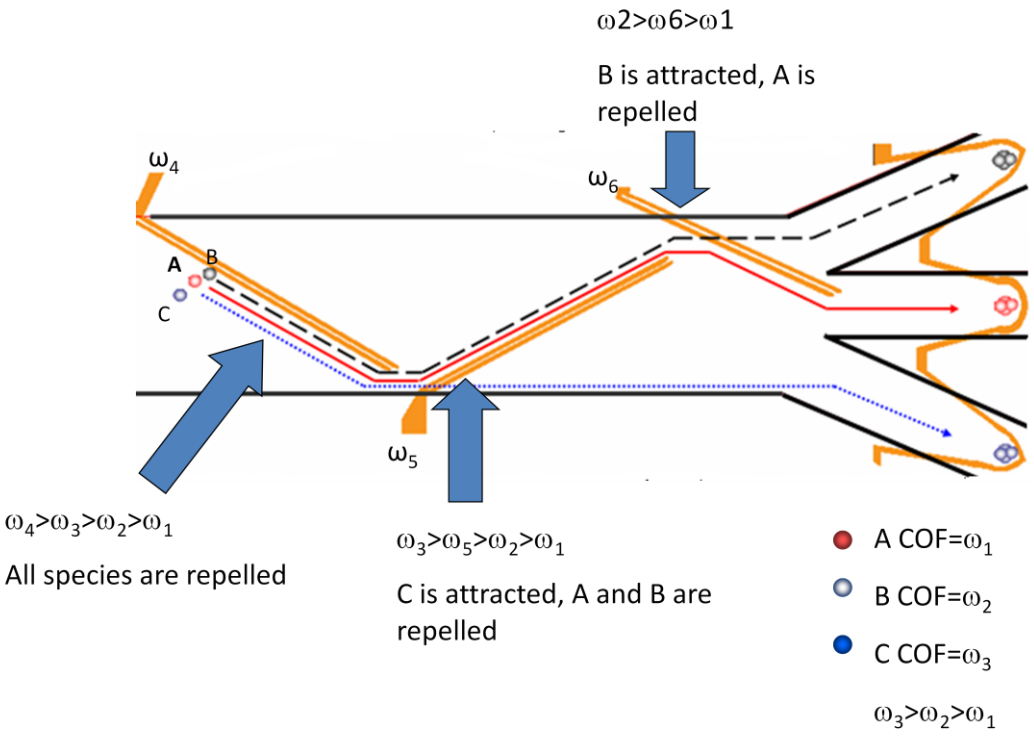

Figure 4.3 Scheme of sorting part

The third part of the chip is the sorting unit. In the current design, this unit has three "3D" electrodes (aligned pairs of electrodes along the top and bottom of the channel). These electrodes are operated at progressively higher frequency. Supposing we have three different kinds of particles to isolate, whose COF frequencies are ω_1, ω_2, ω_3, respectively. In our project, those three particles will be RBC, *E coli* and unwanted particle in blood sample. At the first electrode (that operates at ω_4, which is greater than all the COF of three particles), all three particle types suffer negative DEP and are repelled by the electrodes. In conjunction with the fluid flow field, they traverse a path parallel to the electrodes and are guided to one end of the channel. Here they encounter another 3D electrode gate, –but this one operates at a slightly higher frequency ω_5. At this frequency, one of the particle types suffers positive DEP and is hence dragged toward and through the electrode 'gate", following which it traverses a path along the fluid streamline close to the channel wall and exits through the bottom outlet. The two other particles behave like before and are guided to the other extreme of the channel, where they encounter the third electrode, which operates at a frequency higher than that of the crossover frequency of one of the two remaining particle types. As shown in Figure 4.3, particles of this type are guided to exit from the bottom outlet, whereas the remaining particle type (that suffering negative DEP throughout) is once again repelled and guided out through the central outlet.

The fourth and final stage of the integrated chip is collecting and concentrating the

bacteria after they have been sorted. Due to the high aspect ratio (ratio of width to height) of the channel, the resulting flow profile (commonly referred to as the Hele-Shaw profile) is not parabolic, but exhibits a small boundary layer, whose thickness is roughly equal to the channel height near the side wall where the flow velocity is very small. Therefore, at the sides the particles will suffer the least viscous drag and be influenced most by DEP forces. The 3-D DEP trap electrode has been designed based on this principle. The angling is highest within the boundary layer and quickly curved towards an angled sharp tip. The focusing action of the highly inclined gate at the side and the high field at the tip allows rapid concentration of bacteria to the tip of the trap.

4.2.2. Proposed 2nd generation system

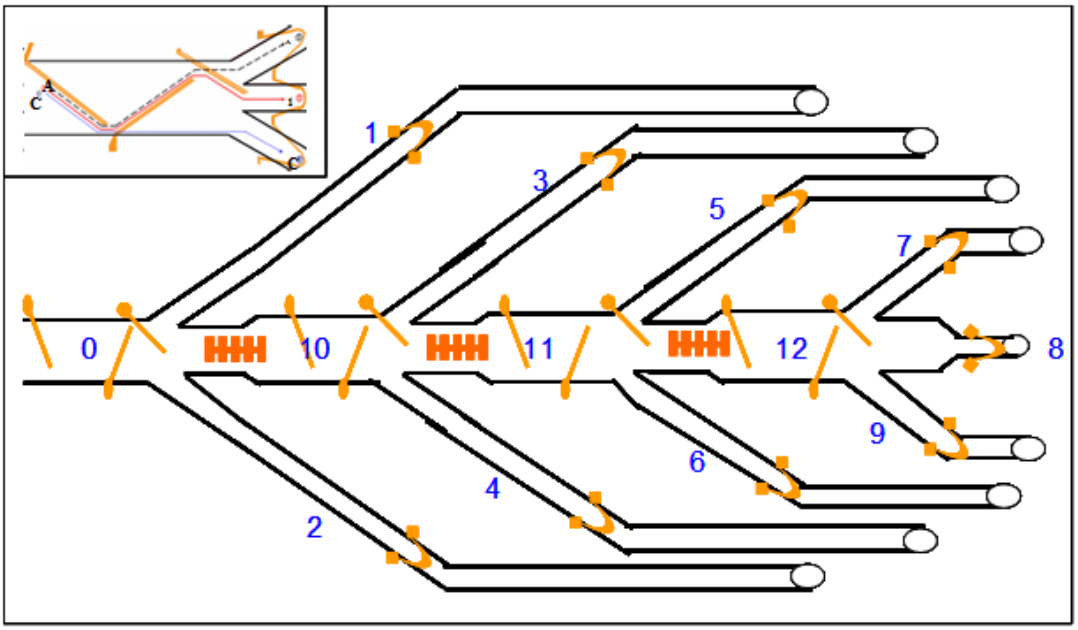

Figure 4.4 Scheme of proposed 2nd generation system

A preliminary design of the proposed microfluidic chip is shown in Figure 4.4. As seen, it essentially consists of the 4 sorter units described in the previous section laid out in series with refocusing units between them. As described in the previous section (and also shown in the inset of Figure 4.4), in each individual sorter unit, the bio-particles with a crossover frequency (COF) lower than that of the second electrode are steered towards the lower outlet; those with a higher COF, but lower than COF of the third electrode are steered into the upper outlet, and particles with the highest COFs exit

through the center. In the proposed design, these particles are fed to the next stage, where the bacterial types with progressively higher crossover frequencies are siphoned away to the top and bottom exits. As with the first generation device, the bacteria steered to the side-channel exits will be collected using a crescent-shaped dielectrophoretic collector operating at a frequency just below that of the electrode guiding the bio-particles into that particular channel.

Since only those particles that display positive dielectrophoresis (pDEP) are steered to the side-channels (marked 1 through 8), particles, such as the non-cellular debris, that are expected to show negative DEP throughout the applied frequency range will pass straight through the device, through exit 9, and subsequently discarded. No particles should be collected at the collection (crescent shaped) electrode at this exit.

Not pictured in the figure is the trap located upstream of the first set of gate electrodes. This trap, as explained in the previous section, captures particles that suffer positive DEP at its operating frequency. If it is desired that the bacterial population should be sorted into more than 8 groups (based on dielectrophoretic mobility), then the trap can be used to collect a large fraction of the bacteria first and then progressively release some particles by gradually changing the applied frequency. For instance, if the trap is operated at a frequency of 10 MHz, only those bacteria with a COF above 10 MHz will pass through to the sorter properly. The gates can then be operated at varying

frequecies from 12 to 24MHz, thus releasing the respective bacteria with COF in those ranges of interest. After that, clear running buffer can be pumped through the system, and the operating frequency of the trap switched to 1 MHz. Now all the bacteria (bio-particles) with COFs between 1 and 10 MHz will be released for sorting and quantification. We believe that the “trap + 4-stage” (8 bio-particle bin) design represents an achievable balance between two demands: turnaround time for the sample and complexity of the device. Alternatively, one can link several of the 4-stage chips depicted in Figure 4.4 in parallel and in series to achieve massively parallel sorting into 20 bins or more. The chips can be linked in a modular fashion and be connected by tubing. The operating frequencies of the sorting gates on each module will, however, vary from chip to chip in order to achieve finer sorting into more bins.

In contrast, a trap and single stage sorter is comparatively easy to design, fabricate and operate. In theory, such a device can be used to sort and quantify bio-particles over a broad range of COFs. The major limitation, however, is that one would have to tolerate long turn-around times as the particles with different COF ranges are sorted and collected one after the other, in series, with respect to time. Putting more stages makes the device overly complicated, especially with respect to balancing fluid flow, and more prone to malfunction (the greater the number of independently operating parts, the greater the chance that at least one of them will malfunction). The 4-stage device proposed in this study is a reasonable size that can eventually be modified into a

hand-held device.

4.3. Design of 4-stage system

A few design issues need to be worked out for the 4-stage sorter. The primary one is to ensure that the fluid flow is not biased towards any of the 9 outlets of the system. This can be ensured by adjusting the dimensions (width and length) of the channel to insure that the total resistance to fluid flow through each of the side channel is the same. Qualitatively, this results in a design where the outlets from the latter stages are run through progressively shorter lengths before the bacteria are trapped and/or the fluid is allowed to drain away.

4.3.1. Laminar flow

Laminar flow, also called streamline flow, occurs when the fluid flows in parallel layers and there is no intermixing between layers.

Reynolds number is the parameter of fluid flow which will always be used to describe flow status. It is given by

$$\mathrm{Re} = \frac{\rho \vartheta D}{\mu} \qquad \text{(Equation 4.1)}$$

where ρ is the density of fluid, ϑ is average velocity in cross section, D is the hydrodynamic diameter of channel, μ is viscosity of fluid (Bird and others 2004).

If the dimensionless Reynolds number of the fluid is less than 2300, it will be considered as laminar flow. Fortunately, because of the extremely small dimension of the MEMS device channel, as well as the flow velocity, the Reynolds number is always much less than 2300, which means the fluid flow in our device is laminar. For example, the flow rate in our device is ~1ul/s, and the cross section is 1.5 mm*50 μm. Supposing the fluid is water, then the Reynolds number in this case will be 13, which is much less than 2300, thus we can say the fluid flow in our device is laminar.

4.3.2. Pressure drop equations

For pressure driven flow in our device, the equation of pressure drop is

$$\Delta P = \rho g \frac{64\mu}{\rho \vartheta D_{eff}} \frac{L}{D_h} \frac{\vartheta^2}{2g} \qquad \text{(Equation 4.2)}$$

Where ΔP is the pressure drop through the channel, g is gravity, D_{eff} is the effective hydrodynamic diameter of channel cross section, D_h is the real hydro diameter of channel cross section, L is the length of channel.

The velocity can be expressed as

$$\vartheta = \frac{Q}{A} = \frac{Q}{WH} \qquad \text{(Equation 4.3)}$$

where Q is the flow-rate, A is the area of cross section, W and H are the width and height of channel, respectively.

The effective and real hydro diameter of channel cross section are given by

$$D_{eff} = \frac{64}{f} D_h = \frac{64}{f} \frac{4A}{P_c} \quad \text{(Equation 4.4)}$$

Where f is the fraction factor, P_c is the perimeter of cross section, which is 2*(W+H) in our device.

The friction factor is related to width/height ratio of cross section, roughly it can be expressed as a function of width and height,

$$f = -50.416(\frac{H}{W})^3 + 132.75(\frac{H}{W})^2 - 121.22\left(\frac{H}{W}\right) + 95.705 \quad \text{(Equation 4.5)}$$

From above equations, we can get

$$\Delta P = \frac{f*(W+H)^2}{8(WH)^3} \mu L Q \quad \text{(Equation 4.6)}$$

4.3.3. Equivalent circuit

The fluid flow in the system is analogous to the flow of the electric current within an electrical circuit. The pressure drop (ΔP) over a section is analogous to the voltage drop over a resistor in electric circuit, the flowrate (Q) is analogous to the current, and the proportionality factor (the rest of equation) is analogous to the resistance. The equivalent circuit is shown in Figure 4.6.

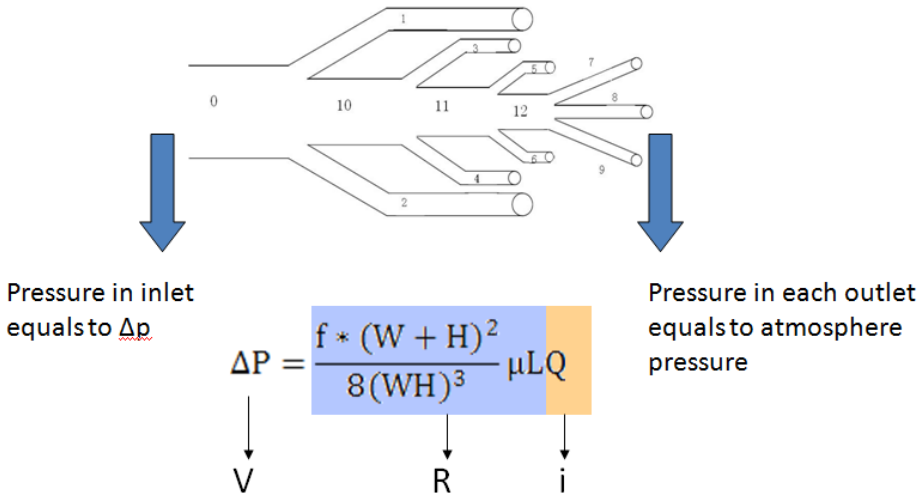

Figure 4.5 Scheme of the pressure drop relationship

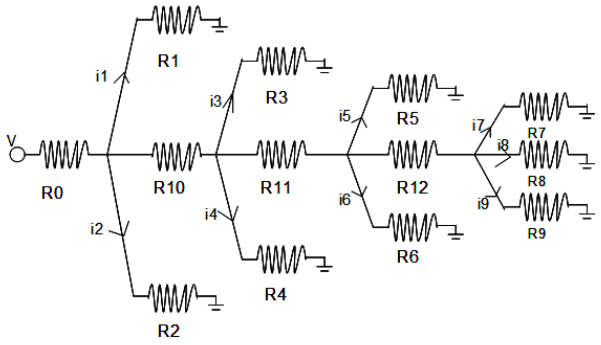

Figure 4.6 scheme of equivalent circuit

In order to get the balanced flow in each outlet, which means $i_1=i_2…=i_9$, we will adjust the resistance of each channel part.

For the sake of making the calculation be easier, the R10, R11 and R12 are set to equal.

$$R_{10} = R_{11} = R_{12} \qquad \text{(Equation 4.7)}$$

It's easy to find out such relationships if the currents are balanced

$$R_7 = R_8 = R_9 \qquad \text{(Equation 4.8)}$$

Applying circuit theory, we obtained the following constraints on the "resitors" in order to have all the currents labeled i_1 to i_9 to be equal to each other.

For example, $i_5*R_5=i_6*R_6=(i_7+i_8+i_9)*R_{12}+i_7*R_7+i_8*R_8+i_9*R_9$

Thus, the constraint is

$$R_5 = R_6 = 3R_{12} + R_7 \qquad \text{(Equation 4.9)}$$

More constraints can be gotten from similar calculations,

$$R_3 = R_4 = 8R_{11} + R_7 \qquad \text{(Equation 4.10)}$$

$$R_1 = R_2 = 15R_{10} + R_7 \qquad \text{(Equation 4.11)}$$

In fluidic terms, the "resistance" of a particular section of the channel is a function of its length, width, and height, and these parameters need to be adjusted to obtain resitances that conform to the constraints above. Since all the sections will be fabricated on the same substrate using Liquid Phase Photopolymerization (Sengupta and others 2002), all the sections will have the same height. The choice of height will be determined in part by the throughput we desire to handle, with larger heights being used for higher volume throughput devices.

Once the height is specified, the other variables are the widths and lengths of individual sections. As seen in Equation 4.6, the resistance happens to scale linearly with respect to length, but in a more complex manner with respect to width. So, from a calculation point of view, it is easier to specify widths of individual sections (with the widths of the daughter channels smaller than that of the mother channels), and calculate the desired lengths for each segment. Values of the width are chosen in a manner than the corresponding lengths obtained are "reasonable" (the system can fit within a larger 6

inch x 8 inch cassette. This is done for one height (100 microns).

The lengths of the channel also determine the location of the electrodes (for the trap, the aligners, the sorter gates and the collectors) and fluidic outlets. We would prefer to be able to use the same set of top and bottom plates to also fabricate channels with different heights. In this case, the lengths are obtained from the previous result, and the widths are calculated to ensure balanced flow.

The trap is a grid, and the aligners are located along the center of the channel. Similarly, the collector collects particles from all regions of the channel and brings them to the center. Hence, they will work as long as the channel is narrower than a certain value. For the sorting gate electrodes to work, they need to convey the particles to a range of streamlines that exit through a desired gate. They are designed such that they either bring the particles to the exact center, or they direct them just barely into the side channels for the the widest channels (that also happen to be the ones with the greatest height). This ensures that they do not span all the way across (and act like a collector) for the narrower channels.

In a specific height circumstance (such as 100μm), we should design the width of each part, and calculate the length, since the relationship between resistance and channel length (linear relation) is much simpler than the relationship between resistance and

channel width.

Another problem we need figure out is, from the above paragraph, we can get the channel length of each part by giving the width, in a specific channel height (for example, 100μm). However, the devices with different heights (such as 25μm, 50μm, 200μm etc) are always needed for research. Then, the 100μm -height device will be used as a template device, to design other similar devices which have different channel heights. We keep the length of each part, and change the width to make the fluid flow in each outlet to be equal. Consequently, we will get a high order equation of width to solve.

4.3.4. Calculation results

A Matlab program is designed for calculation, which will be attached in the appendix of the thesis.

The calculation results are shown in Table 4.1 and 4.2.

Table 4.1 Calculation results of width of each channel

Width of each part (mm)

	1	2	3	4	5	6	7	8	9	10	11	12
Height= 25um	0.1058	0.1058	0.0958	0.0958	0.0588	0.0588	0.0958	0.0958	0.0958	0.6666	0.4529	0.3106
Height= 50um	0.1226	0.1226	0.1125	0.1125	0.0750	0.0750	0.1125	0.1125	0.1125	0.6936	0.4761	0.3310
Height= 100um	0.1500	0.1500	0.1400	0.1400	0.1000	0.1000	0.1400	0.1400	0.1400	0.7000	0.4900	0.3500

Table 4.2 Calculation results of length of each channel

Length of each part: (mm)

	1	2	3	4	5	6	7	8	9	10	11	12
Length (mm)	63.9925	63.9925	39.6883	39.6883	14.7892	14.7892	20.0000	20.0000	20.0000	20.0000	13.4222	13.4222

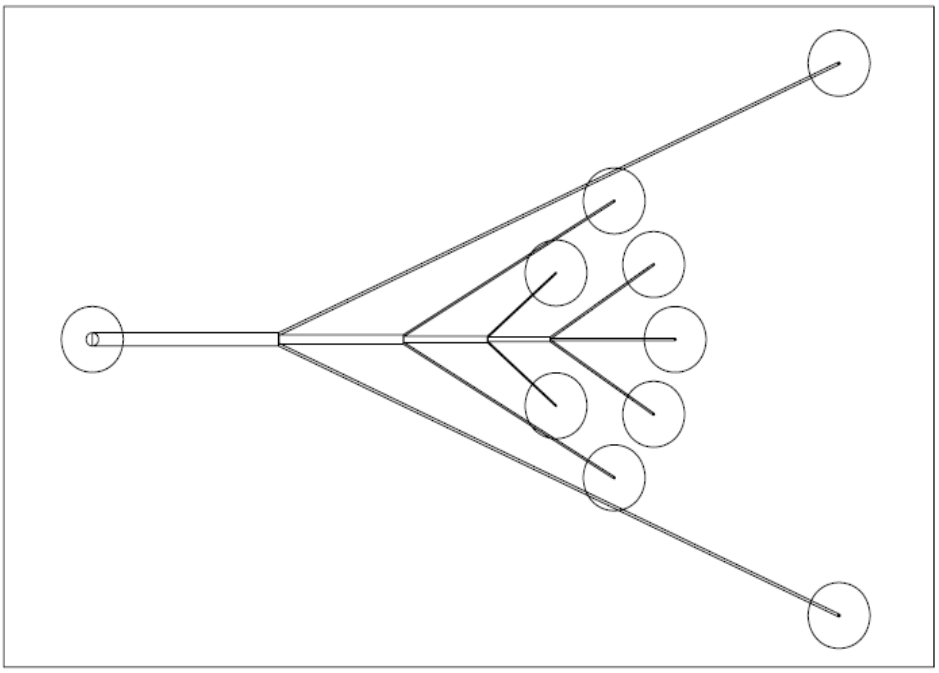

Figure 4.7 CAD channel design of the 2nd generation device, 100µm height.

4.4. Fabrication procedure

4.4.1. Electrodes fabrication

A two-step process is used to fabricate our DEP chip. First, the electrodes were fabricated in Dr. Shubhra Gangopadhyay's lab using photolithography and lift-off on standard 3" x 1" glass slides. The method is summarized in Figure 4.8. We fabricated two designs, one with electrodes that will be located on the upper surface of the chip, and one with electrodes that will be located on the lower surface of the chip. An upper-lower pair was aligned using an optical microscope, and the channels fabricated

using liquid phase photopolymerization (process outlined schematically in Figure 4.9).

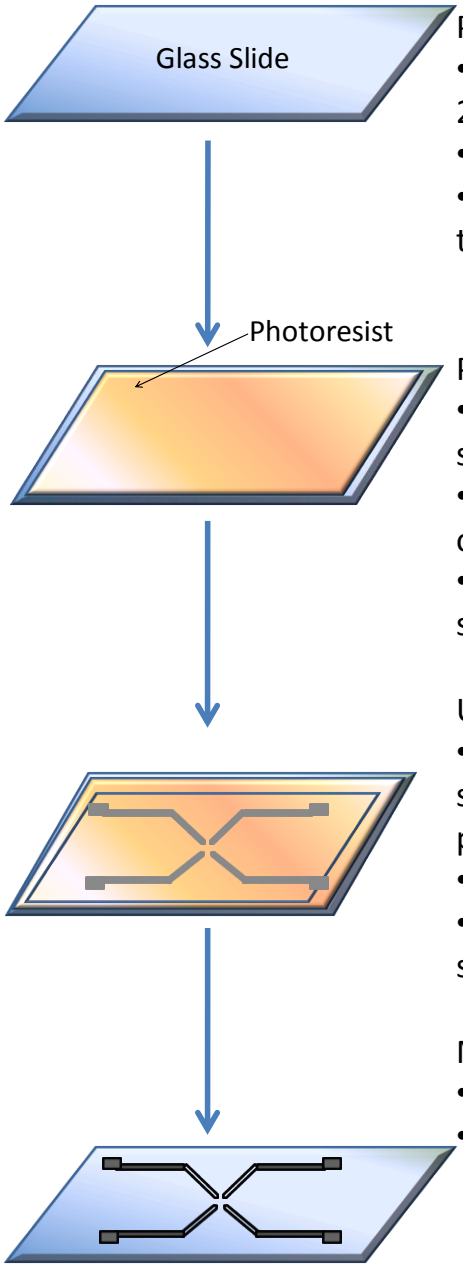

Preparing Glass Slides
•Soak in piranha solution (75% HCl, 25% H2O2)
•Wash with soap and water
•Rinse with acetone, methanol, then isopropynol

Photoresist:
•Spin adhesion promoter onto surface
•Spin negative photoresist (AZ 2020) onto surface
•Soft bake at 115 degrees for 60 sec

UV exposure
•Expose slide to UV light for 4 seconds (time depends on photoresist used)
•Hard bake for another 120 sec
•Develop slides in developer solution (MF 300)

Metal Application
•First layer-titanium
•Second layer-gold

Figure 4.8 Process of electrodes fabrication

4.4.2. Chip fabrication.

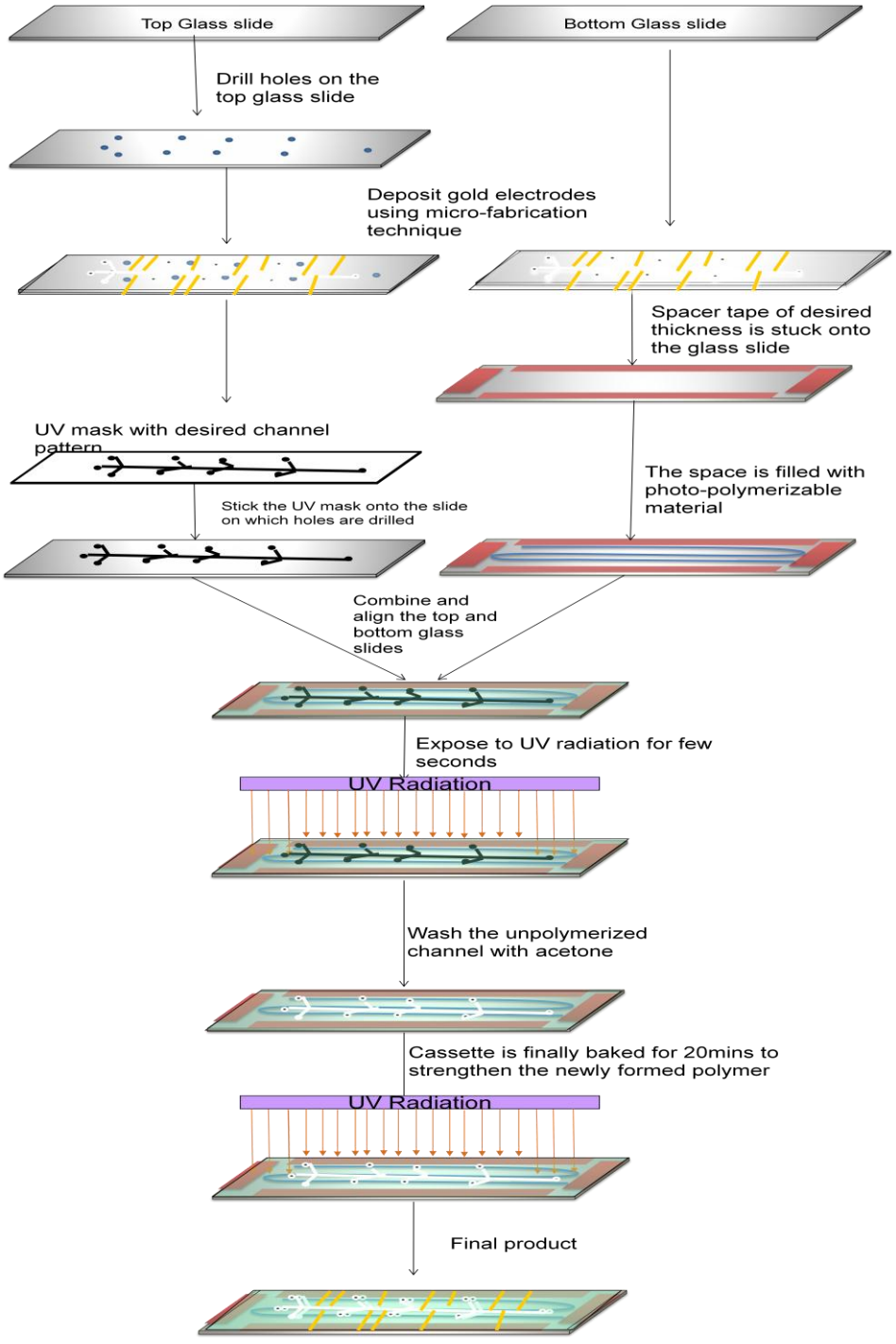

Figure 4.9 Process of electrodes fabrication

4.4.3. Obstacles in 2nd generation chip fabrication

We already made some 1st generation devices; however, the attempt to fabricate the 2nd generation failed. Since the width of the side channels are quite small, it's really hard to wash the unpolymerized channel with acetone, as well as make the accurate width of each channel. In the future the 2nd generation chip may be fabricated using SU-8 or PDMS, which have better mechanical properties, more suitable for the fabrication of fine channels.

CHAPTER 5

FUTURE WORK

The future work includes three major aims:

1. Using the 1st generation device to isolate bacteria from the coarse purified solution by Kinetically Limited Density Deference Centrifugation. Further research like isolation efficiency and bacteria survival rate will be studied in this step.

2. Identification of bacteria isolated by our device using Surface Enhanced Raman Spectroscopy (SERS will be tested).

3. Fabrication and testing of a 2nd generation device by SU-8 or other polymerizable material with better mechanical properties.

APPENDIX

Matlab program of section 4.3

```
function RPL=f1(w,h);% define R=RPL*ul

x=h./w;

y = -50.416.*x^3+ 132.75.*x^2 - 121.22.*x + 95.705;

RPL=y.*(w+h)^2./(8.*(w.*h)^3);


function R=f2(r7,r10)  %given r7 and r12, we can use this function to calculate the other r

r9=r7; r8=r7;

r11=r10; r12=r10;

r1=15.*r10+r7;r2=r1;

r4=8.*r10+r7; r3=r4;

r5=3.*r10+r7; r6=r5;

R=[r1,r2,r3,r4,r5,r6,r7,r8,r9,r10,r11,r12];


W=input('Please enter w1 to w12');

h=input('Please enter channel height');

l7=input('Please enter channel 7 length');
```

```
l10=input('Please enter channel 10 length');
r7=f1(W(7),h).*l7;%calculate the resistance of part 7
r10=f1(W(10),h).*l10;%calculate the resistance of part 10
R=f2(r7,r10);%calculate the resistance of other parts
for (i=1:12)
FPL(i)=f1(W(i),h);
      L(i)=R(i)./FPL(i);
end

w2=zeros(1,12);
a1=-50.416; a2=132.75; a3=-121.22; a4=95.7057;h2=0.025;h=0.1; %the height of this program is 25µm, but we can change the height h2 and constant to get the real solution of the high ordered equation
RPL2=RPL./(0.004*h/h2);    %0.004 is the constant multiplied with RPL
for (j=1:12)

p=[a1.*h2^2/8, a2.*h2/8+a1.*h2/4, a3/8+a2/4+a1/8, a4./(8*h2)+a3./(4*h2)+a2./(8*h2),
a4./(4*h2^2)+a3./(8*h2^2), a4./(8*h2^3), -1*RPL2(j)];
r=roots(p);
r2=r';r3=1./r2;
for (k=1:length(r2))
```

```
        if abs(1./r2(k)-W(j))<0.5*W(j)
                w2(j)=1./r2(k);
        end
end
end

for (i=1:12)
RPL2(i)=f1(w2(i),h2);
        R2(i)=L(i).*RPL(i);
end

t1=R2(10)*15+R2(7); t2=R2(10)*8+R2(7);t3=R2(10)*3+R2(7);
```

REFERENCES

Allain C, Cloitre M, Parisse F. 1996. Settling by cluster deposition in aggregating colloidal suspensions. Journal of Colloid and Interface Science 178(2):411-6.

Angus DC, Linde-Zwirble WT, Lidicker J, Clermont G, Carcillo J, Pinsky MR. 2001. Epidemiology of severe sepsis in the United States: Analysis of incidence, outcome, and associated costs of care. Critical Care Medicine 29(7):1303-10.

Bakken LR. 1985. Separation and Purification of Bacteria from Soil. Applied and Environmental Microbiology 49:1482-7.

Baldwin WW, Kubitschek HE. 1984. Evidence for Osmoregulation of Cell Growth and Buoyant Density in *Escherichia coli*. Journal of Bacteriology 159:393-4.

Balestrazzi A, Bonadei M, Calvio C, Mattivi F, Carbonera D. 2009. Leaf-associated bacteria from transgenic white poplar producing resveratrol-like compounds: Isolation, molecular characterization, and evaluation of oxidative stress tolerance. Canadian Journal of Microbiology 55(7):829-40.

Bird RB, Stewart WE, Lightfoot EN. 2004. Transport Phenomena: John Wiley & Sons, Inc.
Chen DF, Du H, Li WH. 2007. Bioparticle separation and manipulation using dielectrophoresis. Sensors and Actuators, A: Physical 133(2 SPEC. ISS.):329-34.

Cheng IF, Chang HC, Hou D, Chang HC. 2007. An integrated dielectrophoretic chip for continuous bioparticle filtering, focusing, sorting, trapping, and detecting. Biomicrofluidics 1(2).

Dicker DT, Higgins ML. 1987. Cell cycle changes in the buoyant density of exponential-phase cells of Streptococcus faecium. Journal of Bacteriology 169(3):1200-4.
Doern GV, Vautour R, Gaudet M, Levy B. 1994. Clinical impact of rapid in vitro susceptibility testing and bacterial identification. Journal of Clinical Microbiology 32(7):1757-62.

Felice RD, Kehlenbeck R. 2000. Sedimentation velocity of solids in finite size vessels. Chemical Engineering and Technology 23(12):1123-6.

Jacobsen CS, Rasmussen OF. 1992. Development and application of a new method to extract bacterial DNA from soil based on separation of bacteria from soil with cation-exchange resin. Applied and Environmental Microbiology 58(8):2458-62.

Kang CI, Kim SH, Kim HB, Park SW, Choe YJ, Oh MD, Kim EC, Choe KW. 2003. Pseudomonas aeruginosa bacteremia: Risk factors for mortality and influence of delayed receipt of effective antimicrobial therapy on clinical outcome. Clinical Infectious Diseases 37(6):745-51.

Kasai Y, Takahata Y, Manefield M, Watanabe K. 2006. RNA-based stable isotope probing and isolation of anaerobic benzene-degrading bacteria from gasoline-contaminated groundwater. Applied and Environmental Microbiology 72(5):3586-92.

Kneipp K, Haka AS, Kneipp H, Badizadegan K, Yoshizawa N, Boone C, Shafer-Peltier KE, Motz JT, Dasari RR, Feld MS. 2002. Surface-enhanced raman spectroscopy in single living cells using gold nanoparticles. Applied Spectroscopy 56(2):150-4.

Lin M, He L. 2008. Detecting single Bacillus spores by surface enhanced Raman spectroscopy. Sensing and Instrumentation for Food Quality and Safety:247-53.

Loos H, Blok Schut B, Van Doorn R. 1976. A method for the recognition and separation of human blood monocytes on density gradients. Blood 48(5):731-42.

Mancini N, Carletti S, Ghidoli N, Cichero P, Burioni R, Clementi M. 2010. The era of molecular and other non-culture-based methods in diagnosis of sepsis. Clinical Microbiology Reviews 23(1):235-51.

Martinez-Salas E, Martin JA, Vicente M. 1981. Relationship of *Escherichia coli* density to growth rate and cell age. Journal of Bacteriology 147(1):97-100.

Mohd Adnan AF, Tan IKP. 2007. Isolation of lactic acid bacteria from Malaysian foods and assessment of the isolates for industrial potential. Bioresource Technology 98(7):1380-5.

Moskovits M. 2005. Surface-enhanced Raman spectroscopy: A brief retrospective. Journal of Raman Spectroscopy 36(6-7):485-96.

Niederhauser C, Candrian U, Hofelein C, Jermini M, Buhler HP, Luthy J. 1992. Use of polymerase chain reaction for detection of *Listeria* monocytogenes in food. Applied and Environmental Microbiology 58(5):1564-8.

Payne MJ, Kroll RG. 1991. Methods for the separation and concentration of bacteria from foods. Trends in Food Science and Technology 2(C):315-9.

Pohl HA. 1978. Dielectrophoresis. New York: Cambridge University Press.

Savage B, McFadden PR, Hanson SR, Harker LA. 1986. The relation of platelet density to platelet age: Survival of low- and high-density Indium-labeled platelets in baboons. Blood 68(2):386-93.

Schatz GC, Van-Duyne RP. 2002. Electromagnetic mechanism of surface-enhanced spectroscopy. New York: Wiley.

Schiel JE, Hage DS. 2005. Density measurements of potassium phosphate buffer from 4 to 45 C. Talanta 65(2 SPEC. ISS.):495-500.

Sengupta S, Barocas VH, Ziaie B. 2002. Micromachined, Hydrogel-Gated Smart Flow Controller. Digest, Solid-State Sensor and Actuator Workshop:321-4.

Sengupta S, Gordon JE, Chang H-C. 2009. Microfluidic Diagnostic Systems for the Rapid Detectionand Quantification of Pathogens: Springer.

Sorette MP, Galili U, Clark MR. 1991. Comparison of serum anti-band 3 and anti-Gal antibody binding to density-separated human red blood cells. Blood 77(3):628-36.

Tamir H, Gilvarg C. 1966. Density gradient centrifugation for the separation of sporulating forms of bacteria. Journal of Biological Chemistry 241(5):1085-90.

Wenzel RP, Edmond MB. 2001. Severe sepsis - National estimates. Critical Care Medicine 29(7):1472-3.

Willemse-Erix DFM, Scholtes-Timmerman MJ, Jachtenberg JW, Van Leeuwen WB, Horst-Kreft D, Schut TCB, Deurenberg RH, Puppels GJ, Van Belkum A, Vos MC, Maquelin K. 2009. Optical fingerprinting in bacterial epidemiology: Raman spectroscopy as a real-time typing method. Journal of Clinical Microbiology 47(3):652-9.

Yang L, Banada PP, Liu YS, Bhunia AK, Bashir R. 2005. Conductivity and pH dual detection of growth profile of healthy and stressed *Listeria* monocytogenes. Biotechnology and Bioengineering 92(6):685-94.